Nanocell COVID-19 vaccine elicits iNKT-licensed dendritic cells to produce high affinity antibodies neutralizing Variants of Concern

Steven Gao
EnGeneIC Ltd https://orcid.org/0000-0001-5229-1012
Nancy Amaro-Mugridge
EnGeneIC
Jocelyn Madrid-Weiss
EnGeneIC
Nikolina Petkovic
EngeneIC Ltd
Natasha Vanegas
EngeneIC Ltd
Kumar Visvanathan
The University of Melbourne
Vinod Ganju
Peninsula And Southeast Oncology
Gavin Marx
Sydney Adventist Hospital
Bryan Williams
Hudson Institute of Medical Research https://orcid.org/0000-0002-4969-1151
Jennifer MacDiarmid
EnGeneIC
Himanshu Brahmbhatt (hbrahmbhatt@engeneic.com)
EnGeneIC Pty Ltd

Article

Keywords:

Posted Date: April 7th, 2022

DOI: https://doi.org/10.21203/rs.3.rs-1472661/v1

Abstract

For COVID-19 vaccines, high-affinity antigen-specific antibody, CD8+ T cell and memory B cell responses are essential to maximize protection against Variants of Concern (VOC). We report results in vitro, in mice and human volunteers immunized with bacterially-derived, non-living nanocells (EDVTM) packaged with bacterial plasmid expressing spike protein of SARS-CoV-2 and IFNγ stimulating adjuvant α-galactosylceramide (EDV-COVID-αGC). EDV-COVID-αGC is shown to elicit iNKT-licensed dendritic cell activation/maturation, follicular helper T cell cognate help to B cells to undergo germinal center based somatic hypermutation and production of high affinity antibodies able to neutralize Alpha, Beta, Gamma, Delta, and Omicron VOC including a memory B cell response. Type I and Type II interferon stimulation and S-specific CD8+ T cells was also achieved. EDV-COVID-αGC are lyophilized, stored and transported at room temperature.

Introduction

SARS-CoV-2 (Severe Acute Respiratory Syndrome-Coronavirus type 2) is the causative agent of the COVID-19 pandemic and despite global vaccination efforts the pandemic is failing to abate, particularly with the continuous emergence of VOC. Structurally, SARS-CoV-2 has 4 proteins; Spike (S), Envelope, Membrane and Nucleocapsid [1]. S-protein Receptor Binding Domain (RBD) binds to human angiotensin-converting enzyme 2 (hACE2) receptor on host cells [2], and is responsible for cell attachment and fusion during viral infection. S-protein is 1273 amino acids (aa) in length and consists of a signal peptide (1–13 aa) located at the N-terminus, the S1 subunit (14 – 685 aa) comprising an N-terminal domain (14–305 aa) and RBD (319–541 aa), and the S2 subunit (residues 686–1273 aa) [3]. RBDs are key neutralization targets and current vaccines primarily aim to elicit RBD-specific neutralizing antibody and T cell responses [4].

For vaccines to be successful, the host requires a robust immune system which is sub-optimal in immune-compromised patients e.g., cancer, HIV, and hence these patients remain vulnerable to SARS-CoV-2 and VOC [5-8]. Furthermore, there are logistical issues since currently approved vaccines need to be stored and transported at -20^{o}C to -70^{o}C with a shelf-life of only three to six months.

Here we describe a novel class of vaccine, designated EDV-COVID-αGC, comprising a 400nm diameter, non-living, achromosomal nanocell, EDV^{TM} (EnGeneIC Dream Vector) packaged with (i) Type I interferon stimulating bacterial gene expression recombinant plasmid carrying S-protein encoding sequence, (ii) plasmid expressed S-protein produced in the nanocell cytoplasm, and (iii) Type II interferon stimulating glycolipid adjuvant αGC (Fig. 1A). EDVs are derived from a mutant non-pathogenic *Salmonella typhimurium* bacterium that buds off the bacterium during its normal replication due to asymmetric cell division induced by the chromosomal mutation [9, 10]. Single chain Fv bispecific (scFv) antibody-targeted EDVs have been used to deliver cytotoxic payloads and small molecules to solid cancers in Phase I and IIa clinical trials in several solid tumors. Tumor stabilization/regression, prolonged overall survival, and

minimal to no toxicity despite repeat dosing, has been achieved in these patients who had exhausted all treatment options [11-13].

This work shows that EDV-COVID-αGC can deliver SARS-CoV-2 S-protein and αGC to dendritic cells (DCs) setting off a S-specific humoral and cellular response with broad-spectrum neutralization against Wild Type, Alpha, Beta, Gamma and Delta variants at greater than 90% and Omicron variant at greater than 70%. Furthermore, we present results of the first 4 volunteers of the EDV-COVID-αGC Phase I clinical trial which encouragingly echo our pre-clinical data thus far.

Results

SARS-CoV-2 EDV formulation and dual antigen presentation

As previously published, cancer therapeutic EDVs are packaged with a cytotoxic payload and targeted to cancer cells via scFv bispecific antibodies specific to EDV lipopolysaccharide and cancer cell receptors such as EGFR [9]. In this study, we created EDV-COVID-αGC, a dual packaged nanocell carrying both the SARS-CoV-2 spike protein and the glycolipid adjuvant, α-galactosylceramide (Fig. 1A). The pLac-CoV2 bacterial recombinant plasmid expressing SARS-CoV-2 S-protein under a modified β-lactamase promoter (Fig. 1B), was transformed into the EDV producing *S. typhimurium* and purified EDV-COVID nanocells were shown to contain both subunits of the S-protein by western blot using a polyclonal antibody against S1 and a monoclonal antibody against the S2 subunit (Fig. 1C). EDV plasmid extraction and quantitation gave a plasmid copy number of ~100 copies pLac-CoV2 per EDV (Table S1) whilst protein quantitation showed ~16ng of spike protein per 10^9 EDVs (Fig. S1).

Purified EDV-COVID were loaded with αGC to produce EDV-COVID-αGC and LC-MS/MS measurement from lipid-extracted EDV-COVID-αGC showed ~30 ng of αGC per 10^9 EDV's (Fig. 2S). Flow cytometric analysis of murine JAWS II cells treated with EDV-COVID-αGC and stained with anti-CD1d:αGC demonstrated the uptake and CD1d mediated surface presentation of αGC (Fig. 1D). Furthermore, co-staining of JAWS II cells with anti-spike S1 and anti-CD1d:αGC, confirmed the presentation of both S-protein and αGC on the surface of DCs following co-incubation with EDV-COVID-αGC (Fig. 1E).

Early cytokine response in mice treated with EDV-COVID-αGC

Intramuscular (i.m.) inoculation of BALB/c mice with a single first dose of 2 x 10^9 or 3 x 10^9 EDV-COVID-αGC resulted in 8 h serum samples showing elevated Th1 cellular immune response cytokines compared to controls. As shown in Fig. 1 (F-K), IFNα, IFNγ, IL-12p40, IL-2, TNFα, and IL-6 rose to significantly higher levels in EDV-COVID-αGC groups compared to controls including Saline, EDV, EDV-CONTROL (spike-negative plasmid) and EDV-COVID (spike protein alone), demonstrating the impact of αGC. IL-21, a Th2 cytokine crucial in anti-viral activity was significantly elevated in mice treated with EDV-COVID-αGC by 8 h (Fig. 1L). IL-10, also a Th2 cytokine was elevated comparatively among all groups (Fig. 1M).

S-protein-specific antibody titers in mice treated with EDV-COVID-αGC

Mice dosed i.m. with 2 x 10^9 or 3 x 10^9 EDVs and an equal boost at day 21 were analyzed for serum IgM and IgG antibody titers at day 28 using S-protein-specific ELISA. Both dose levels of EDV-COVID and EDV-COVID-αGC gave elevated IgM (Fig. 2, A and C) and IgG (Fig. 2, B and D) S-protein-specific antibody titers compared to Saline, EDV and EDV-CONTROL groups. Antibody titers were higher for EDV-COVID-αGC compared to EDV-COVID. IgM (Fig. 2E) and IgG (Fig. 2F) levels were shown to be elevated by day 7 at comparable levels for both EDV-COVID and EDV-COVID-αGC. By day 21 prior to boosting, IgM titers dropped for both EDV-COVID and EDV-COVID-αGC groups (Fig. 2G) but remained elevated for IgG, particularly in the EDV-COVID-αGC group (Fig. 2H).

S-protein-specific B and T cell response

To study the B cell response after immunization of mice at both 2 x 10^9 and 3 x 10^9 levels, bone marrow derived B cells were stimulated *ex-vivo* with SARS-CoV-2 S-protein and B cell secreted S-specific IgM and IgG titers were measured. A dose of 2 x 10^9 EDV-COVID-αGC resulted in significantly elevated IgM and IgG levels (p=0.0081, p<0.0001) compared to all other groups dosed at 2 x 10^9 and similarly, 3 x 10^9 EDV-COVID-αGC resulted in significantly elevated IgM and IgG levels compared to all other groups at 3 x 10^9 (p<0.0001, p=0.0175) (Fig. 3, A and B).

When analyzing the activation marker CD69 as a percentage of CD3/CD69 within the *ex vivo* splenic $CD8^+$ T cell population by flow cytometry, a dose of 2 x 10^9 EDV-COVID-αGC gave a higher T cell response (p=0.0159) following stimulation with S-protein compared to DMSO stimulation (Fig. 3C). This higher % CD3/CD69 ratio was also observed at a dose of 3 x 10^9 (p=0.0185) (Fig. 3D).

In Fig. 3E, Th1/Th2 phenotyping studies following S-protein stimulation of *ex-vivo* splenocytes, show that CD4+ T cells from EDV-COVID and EDV-COVID-αGC mice produced IFNγ but not IL-4 within 24 h compared to other groups, which had no response.

Multi-strain neutralization by EDV-COVID-αGC measured using a Surrogate Viral Neutralization Test (sVNT)

FDA approved cPASS™ sVNT kit was used to evaluate the level of neutralizing antibodies in mouse serum at day 28 post i.m. inoculation of 2 x 10^9 and 3 x 10^9 (for Wild type Wuhan strain) and 3 x 10^9 for Alpha, Beta, Gamma and Delta strains. According to the kit's specifications a sample is deemed positive for neutralization at 30% level of inhibition [14, 15]. Following these guidelines, at a dose of both 2 x 10^9 and 3 x 10^9, 100% of the mice treated with EDV-COVID-αGC neutralized RBD from Wild type SARS-CoV-2, while 50% and 75% respectively for the corresponding doses of EDV-COVID showed RBD neutralization (Fig. 3, F and G). 100% of mice treated with 3 x 10^9 EDV-COVID-αGC neutralized the respective RBDs from Alpha strain, 80% Beta and 90% Gamma and Delta (Fig. 3, H-K).

EDV-αGC in cancer patients

EDV-αGC have been administered to humans in an on-going Phase I/IIa clinical trial in pancreatic cancer and EGFR-expressing end-stage cancer patients receiving EGFR-targeted, cytotoxic drug PNU-159682 packaged EDVs plus EDV-αGC (https://www.anzctr.org.au/Trial/Registration/TrialReview.aspx?id=365258&isReview=true. Fig. 4A shows a typical finding from over 800 doses of EDV-αGC thus far in these cancer patients, where 3 h post-dose with EDV-αGC, there is an increased lymphocyte count. Our interim pancreatic patient results also demonstrate that TNFα and IL-6 spike 3 h post-dose and that the levels do not surpass the physiologically normal range with repeat dosing (Fig. 4, B and C).

Data from the first 4 volunteers in EDV-COVID-αGC clinical trial.

PBMC analysis showed that there was an increase in CD4/CD8 co-positive T cells by day 28 post-initial injection with day 21 booster, compared to that on day 1 (Fig. 5A). The $CD4^+/CD8^+$ T cells are thought to have anti-viral capabilities [16]. PBMCs from day 28 had an elevated number of $CD69^+$ T cells compared to PBMCs from day 1. In addition, when stimulated with the SARS-CoV-2 S-protein, a further increase in CD69 expressing T cells was observed in day 28 samples but not in day 1 samples (Fig. 5B). The amount of virus-specific effector follicular helper T (T_{FH}) cells, which are identified as $CD4^+$ $CCR7^{lo}$ and $PD1^{hi}$, and are thought to be responsible for IL-21 production [17], were increased following vaccination on day 28 (Fig. 5C). There was also a dramatic increase in the amount of $CCR7^+$ $CD27^+$ central memory T cells within the $CD4^+$ $CD45RA^-$ PBMC population on day 28 compared to day 1 (Fig. 5D). A similar degree of increase was also observed in $CD4^+$ $CD45RA^-$ $CCR7^+$ $CD27^+$ central memory T cells (Fig. 5E). B cell analysis also showed that there's a marked increase in naïve B cells and plasmablasts on day 28 compared to day 1 (Fig. 5F).

When stimulated with the SARS-CoV-2 S-protein, PBMCs taken from volunteers on day 28 post-initial injection produced IFNγ. Antigen specific IFNγ production was not observed from PBMCs taken on day 1 pre-injection (Fig. 5G). IL-21 was also produced constitutively by *ex-vivo* PBMCs taken on day 28 but not by those taken on day 1 (Fig. 5H). Interestingly, the supernatant from SARS-CoV-2 S-protein and to a lesser extent, PHA stimulated PBMCs taken on day 28 had neutralizing effect against viral RBD binding to hACE2 protein, while the same phenomenon was not observed from day 1 PBMCs. The neutralization effect of PBMCs is sustained for at least 3 months post-initial injection (Fig. 6A).

cPASS™ surrogate neutralization tests revealed that by day 28, the serum of all 4 healthy volunteers contained high levels of neutralizing antibodies that were equally effective against all the SARS-CoV-2 variants tested with only a slight reduced efficacy against Omicron, which has been shown to be particularly difficult to neutralize (Fig. 6B). The serum samples needed to be diluted on average 435 times before falling below the 30% cut off of the cPASS assay against the wildtype virus (Fig. 6C). In the four volunteers presented here, serum IFNγ rose by day 21 and remained elevated at 3 months (Fig. 6D).

Discussion

Despite an unprecedented global effort over two years to curb the COVID-19 pandemic, the effort is frustrated by the continuous emergence of VOC resulting in the decline of vaccine protective efficacy to various degrees. Additionally, the current vaccines demonstrate limited protective efficacy in immune-compromised population such as those with cancer, HIV, organ transplant and autoimmune diseases. Logistic issues such as the requirement to store and transport vaccines at -20^{o}C to -70^{o}C and a shelf life of only 3 to 6 months makes it difficult to get these vaccines to rural populations especially in Africa.

Here we provide data on a novel COVID-19 vaccine that readily overcomes these limitations.

The vaccine comprises a 400nm non-living, achromosomal nanocell (EDV; EnGeneIC Dream Vector) derived from a non-pathogenic strain of *Salmonella typhimurium*. The bacterial strain carries a mutation that results in asymmetric cell division during normal bacterial cell division where the EDVs bud off at the poles of the mutant bacteria [9]. The purified EDVs are pre-packaged with a bacterial gene expression recombinant plasmid carrying the SARS-CoV-2 S-protein encoding gene under a constitutive gene expression, modified β-lactamase promoter (EDV-COVID). The plasmid expresses the S-protein in the bacterial cytoplasm during normal bacterial growth and when the EDV is formed, a significant concentration of the S-protein segregates into the EDV cytoplasm. Additionally, the EDV-COVID nanocells are further packaged with αGC (EDV-COVID-αGC). 10^9 EDVs were shown to carry ~16ng of S-protein, ~30ng of αGC and ~100 copies of plasmid per EDV (Fig. S1-S2).

Previous studies had shown that post-systemic administration, EDVs are phagocytosed by professional phagocytic cells such as macrophages and DCs and are degraded in lysosomes releasing the drug, nucleic acid, or adjuvant payload into the cytoplasm [9]. Flow cytometry studies showed that EDV-COVID-αGC effectively delivered both S-polypeptides and αGC into murine bone marrow derived JAWSII DCs and that αGC was presented on the DC surface through glycolipid antigen presenting MHC Class I-like molecule, CD1d, to a similar efficiency as free αGC (Fig. 1D). The same DCs also presented S-polypeptides likely via MHC Class II molecules on the cell surface (Fig. 1E).

The display of αGC:CD1d on the DC cell surface recruits iNKT cells which carry the invariant TCR that is known to bind to CD1d-associated αGC on DCs, resulting in rapid secretion of IFNγ [18] as seen in only the EDV-COVID-αGC group of mice (Fig. 1G). Serum IFNγ release was sustained even 3 months post-vaccination in the 4 human volunteers (Fig. 6D) suggesting activation of iNKT cells via the αGC:CD1d display on APCs (Fig. 4D). In contrast the currently approved mRNA vaccine (BNT162b2) showed transient serum IFNγ release which wanes by day 8 [19]. This is not surprising since the mRNA vaccines do not elicit antigen-specific antibodies via the iNKT/DC pathway. This iNKT cell activation and IFNγ secretion is critical in the activation of the high-affinity antibody production pathway depicted in Fig. 4D.

The DCs engulfing the EDVs are further activated via the pathogen associated molecular patterns (PAMPs) like EDV-associated LPS [20]. This activation releases TNFα which is evident in all four EDV containing groups (Fig. 1J).

It has been demonstrated that activated iNKT cells promote DC maturation via CD40/40L signaling and cytokines IFNγ and TNFα [21]. It is also established that DCs express co-stimulatory molecules CD80/86 but after activation by iNKT cells, expression of these molecules is rapidly upregulated as seen in our cancer studies (data not shown). Upregulation of CD40L on DC surface induces their maturation and secretion of IL-12 (Fig. 1H). Once more, the secretion of IL-12 was only observed with the EDV-COVID-αGC group. This promotes the cytolytic function of cytotoxic CD8+ T cells and priming of CD4+ T cells [22] to provide cognate help to B cells for antibody production.

Splenic CD8+ cytotoxic T cells from mice immunized with EDV-COVID-αGC exhibited the highest number of CD3+/CD69+ cytotoxic T cells compared to those in all other groups (Fig. 3, C and D). T cell responses are important for both early viral clearance and long-term protection through memory S-specific T cells [23]. This data suggests that EDVs carrying S-protein were able to induce CD8+ T cell specificity, further enhanced by the inclusion of αGC.

It has been established that B cells that have MHC Class II presented protein antigen first engage in cognate interactions with T_{FH} cells at the junction between the T cell–rich areas and B cell follicles of secondary lymphoid tissues [24-26]. Engagement of MHC Class II/antigen complex on these B cells with the T_{FH} cell surface TCR results in the rapid upregulation of cognate helper co-stimulatory molecules CD40L [27], inducible T cell co-stimulator ICOS [28] and PD-1 (Fig. 4D).

Binding of ICOS ligand which is expressed on naive B cells [29], to ICOS on T_{FH} cells is essential for the progression of pre-T_{FH} to fully differentiated T_{FH} cells. ICOS/ICOSL signalling also leads to the release of multiple cytokines including IFNγ, IL-4, IL-10, IL-17, IL-2, IL-6 and IL-21 [30-33].

IL-6 has been shown to promote differentiation of activated CD4+ T cells into T_{FH} cells during an immune response. IL-6 was shown to be elevated in the EDV-COVID-αGC injected group compared to all the controls (Fig. 1K). Secretion of TNFα and IL-6 (Fig. 1, J and K) was short lived, self-limiting and none of the mice experienced any observable side effects.

IL-10 also has anti-inflammatory properties playing a key role in limiting host response to inflammatory cytokines like TNFα. IL-10 is part of the innate immune response to the EDV associated LPS and hence occurred to the same extent (Fig. 1M) in all the EDV containing groups.

Splenocytes from mice immunised with EDVs when stimulated with S-protein trimer showed that CD4+ T cells from EDV-COVID and EDV-COVID-αGC mice, but not those from other groups produced IFNγ but not IL-4 (Fig. 3E) indicating that $CD4^+$ T cells were primed to elicit an antigen specific Th1 type response following vaccination.

IL-21 is mainly expressed by T_{FH} cells and stimulates the proliferation of B cells and their differentiation into plasma cells. Class switching to IgG and IgA of CD-40L-interacting B cells is also promoted by IL-21 [34].

A highly significant increase in IL-21 only in EDV-COVID-αGC treated mice was also observed (Fig. 1L) suggesting that αGC in EDV-COVID was essential to activate CD4+ T_{FH} cells likely due to iNKT-licensed DC activation of T_{FH} cells as described above. Similarly, PBMC's from the 4 volunteers when spiked with S-protein showed that on day 28 there was a significant increase in IL-21 secretion (Fig. 5H). In terms of S-specific antibody responses, IL-21 plays a critical role in T cell–dependent B cell activation, differentiation, germinal center (GC) reactions [35] and selection of B cells secreting antigen-specific high affinity antibodies. IL-21 secretion in humans receiving the mRNA vaccines has not been reported.

B cell activation results in either the extrafollicular proliferation of long-lived antibody producing B cells as plasmablasts or their entry into GCs for the subsequent development of memory or plasma cells [36]. Post-T_{FH} cell cognate interactions in the follicles, proliferating B cells give rise to GCs and undergo somatic hypermutation (SHM) in their immunoglobulin V-region genes and affinity maturation which produces plasma and memory cells of higher affinity [37-43]. Within the GC, T_{FH} cells provide further B cell help mainly through the secretion of IL-21 and CD40L co-stimulation, which are two major factors for B cell activation and differentiation. IL-21 also induces class switching to IgG1 and IgG3 by human naive B cells and increased secretion of these Ig isotypes by human memory B cells [44].

B cells isolated from mouse bone marrow at 28-day post-initial injection when co-incubated with S-protein showed that B cells from EDV-COVID-αGC immunized mice produced significantly higher levels of S-specific IgM (Fig. 3A) and IgG (Fig. 3B) compared to all other groups. This indicates that EDV-COVID-αGC treatment induced SARS-CoV-2 specific memory B cells that could respond rapidly to S-protein re-exposure.

Increase in circulating naïve B cells and plasmablasts post-vaccination showing that the B cells in vaccinated individuals are actively differentiating towards memory B cells following antigen exposure was shown in the four human volunteers at 28 days post-vaccination (Fig. 5F). Transition towards memory B cells from naïve B cells to plasmablasts has not previously described for mRNA vaccines.

At both dose levels, high levels of anti-S protein IgM (Fig. 2, A and C) and IgG (Fig. 2, B and D) antibody titers were detected in the serum of most mice immunized with EDV-COVID-αGC at 28 days post-initial dose and a booster dose at day 21. IgM and IgG antibodies were also elicited by mice immunized with EDV-COVID but the IgG response was lower (Fig. 2, A-D). The inclusion of αGC into EDV-COVID resulted in a dramatic and consistent elevation of S-specific IgG titers. S-specific IgG responses by days 7 and 21 with EDV-COVID and EDV-COVID-αGC were similar (Fig. 2, F and H) however, the booster effect was pronounced on day 28 only in EDV-COVID-αGC immunized mice suggesting that the inclusion of αGC is likely to have directed the EDV-COVID-αGC towards the iNKT-licensed DC pathway, known to result in germinal center B cell activation/maturation with high titer antibody secretion.

Interestingly EDV-COVID would not be expected to elicit S-specific antibodies via the iNKT/DC/T_{FH} pathway and hence would not be expected to elicit the immunoglobulin class switching from the initial IgM response to IgG as would be expected via the iNKT/DC/T_{FH} pathway elicited by EDV-COVID-αGC.

Surrogate virus neutralization tests showed 100% of the mice immunized with EDV-COVID-αGC were positive for neutralizing antibody against the wild type SARS-CoV-2 virus (Fig. 3, F and G). In contrast, neutralizing antibodies were only detected in 50% (Fig. 3F) and 75% (Fig. 3G) of the mice immunized with EDV-COVID, highlighting the importance αGC in this vaccine. When tested against 4 common SARS-CoV-2 variants, Alpha (B.1.1.7), Beta (B.1.351), Gamma (P.1) and Delta (B.1.617.2), mice immunized with 3 x 10^9 EDV-COVID-αGC strongly neutralized binding of Alpha (100%; Fig. 3H), Beta (80%; Fig. 3I), Gamma (90%; Fig. 3J) and Delta (90%; Fig. 3K) S-proteins. In contrast, EDV-COVID poorly neutralized Alpha (50%; Fig. 3F), Beta (0%; Fig. 3I), Gamma (40%; Fig. 3J) and Delta (50%; Fig. 3K) variants.

Similar results were seen in the 4 healthy human volunteers (Fig. 6A) where the $PRNT_{90}$ (90% reduction in binding of the respective RBD to hACE2) virus neutralization of the serum antibodies at day 28 showed strong neutralization of RBDs from Wuhan (100%), Alpha (100%), Beta (100%), Gamma (100%), Delta (100%) and Omicron (75%). In contrast the data for the mRNA vaccine (BNT162b2) was only provided for the $PRNT_{50}$ assay (requires only 50% neutralization of RBDs) and these results required a serum dilution reduction of 2-fold (Alpha), 5 to 10-fold (Beta), 2 to 5-fold (Gamma), 2 to 10-fold (Delta), to achieve $PRNT_{50}$ [45] and over 22-fold for Omicron [46].

In the presence of T cell help, B cells reacting to protein antigens can either differentiate into extrafollicular plasma cells, giving rise to a rapid wave of low-affinity antibody, or grow and differentiate in follicles, giving rise to germinal centres. The data from sVNT show that the antibodies elicited via EDV-COVID-αGC are able to provide high level of neutralization of the RBDs from VOC suggesting that these are high affinity antibodies likely due to the entry of B cells into GCs and undergoing SHM resulting in high affinity antibodies. In contrast, antibodies generated by EDV-COVID immunisation did not afford protection against the VOC RBDs suggesting that these B cells did not receive full cognate T_{FH} help resulting in the formation of released plasma cells producing low affinity antibodies that were ineffective against the VOC RBDs.

In an on-going Phase I/IIa clinical trial in pancreatic cancer and EGFR-expressing end-stage cancer patients who are being administered EGFR-targeted, PNU-159682 (cytotoxic drug) packaged EDVs plus EDV-αGC, the interim results show that despite the severely immune-compromised state of the patients, 3 h post-dose, there is a significant activation, maturation and proliferation of lymphocytes (Fig. 4A). Lymphopenia is commonly observed at the COVID-19 disease onset [47]. Similarly, 3 h post-dose, TNFα (Fig. 4B) and IL-6 (Fig. 4C) levels also spiked and despite repeat dosing, these levels remained within physiologically normal levels. Over 800 doses of EDV-αGC have been administered in these patients and despite repeat dosing, with many patients receiving 15 to 70 repeat doses of EDV-αGC, no toxic side effects have been observed.

This data suggests that the EDV-COVID-αGC vaccine may have the potential for early activation of the immune system with a broad anti-viral immune response even in the highly immunocompromised population and may assist in withstanding the occurrence of severe lymphopenia in these patients if they were to get infected with SARS-CoV-2 or its variants.

PBMC analysis from 4 healthy volunteers from our Covid vaccine phase I clinical trial showed that by day 28 post-initial vaccination and day 21 booster dose, there's an increase in CD4/CD8 co-positive T cell population in the PBMCs (Fig. 5A), which has been shown to have a memory phenotype and may differentiate into effector cells producing high amount of IFNγ following antigen exposure [16]. The increase of this population of T cells has not been described by studies of other vaccines. In addition, there were more $CD69^+$ $CD8^+$ and $^-CD69^+$ $CD8^-$ T-cells by day 28 post-initial injection and the number of $CD69^+$ T cells in the *ex vivo* PBMCs further increased following S-protein stimulation (Fig. 5B). This indicates that the population of circulating T cells were SARS-CoV-2 antigen specific, as observed with other vaccines [48].

Furthermore, a notable increase in $CD4^+$ and $CD8^+$ central memory T cells were observed by day 28, as well as effector T_{FH} cells and in turn, an increase in the number of naïve B cells and plasmablasts suggesting that the immune system was going through antigen specific T cell and subsequent B cell activation as indicated in Fig 4D. Moreover, by day 28, IL-21 was produced constitutively by *ex-vivo* PBMCs (Fig. 5H) and IFNγ could be detected in the supernatant of PBMCs (Fig. 5G) stimulated with the SARS-CoV-2 spike protein, which corroborate the proposed pathway (Fig. 4D). Interestingly, the supernatant of day 28 *ex-vivo* PBMCs stimulated by the S-protein had the ability to neutralize SARS-CoV-2 binding to hACE2, as determined using the cPASS assay. This was not observed in the unstimulated PMBCs nor in day 1 samples, demonstrating that the circulating lymphocytes in the immunised volunteers had the ability to detect SARS-CoV-2 antigen and produce antibodies that inhibits RBD to hACE2 binding in response to that exposure. This ability for *ex vivo* PBMCs to produce neutralization antibodies was sustained for at least 3 months (Fig. 6A). This, to our knowledge has not yet been described in other vaccine studies.

Analysis of serum neutralizing antibodies of the 4 volunteers showed that the level of neutralizing antibody titers against the wildtype virus on day 28 was consistent or better than some of the currently available vaccines[14]. Similar to the finding from our mouse experiments, the serum of the 4 volunteers showed remarkable consistency of neutralization abilities when tested against 4 of the common VOC as well as the wildtype of the virus (Fig. 6, B-C), with high neutralizing titers. Our neutralizing results are combined with elevated serum IFNγ extending to 3 months (Fig. 6D).

It is currently thought that successful vaccination relies on both antibody- and T cell-mediated immunity and while it is recognized that at least Type I and Type II interferons can elicit a broad anti-viral immunity, due to the multitude of effects that these interferons exhibit, it is quite possible that to curb the current and future viral pandemics, a broad specific and non-specific anti-viral immunity combined with a specific memory B and T cell response may be necessary.

Of greater importance is the type of antibodies that are elicited by the vaccine. Most vaccines do not elicit the iNKT-licensed DC pathway and hence the B cells rapidly release low affinity antibodies which then fail to neutralize VOC RBDs. In contrast, the iNKT-licensed DC pathway elicits high affinity antibodies due to B

cells undergoing affinity maturation and SHM in GCs and these high affinity antibodies can be highly effective in neutralizing VOC RBDs.

EDV based cancer therapeutics or COVID vaccines are lyophilized post-manufacturing and can be stored and transported world-wide at room temperature. The shelf life of EDV cancer therapeutics have currently been shown to be over 3 years and the EDV-COVID-αGC vaccine has exceeded 1 year of stability.

Materials And Methods

Recombinant CoV proteins and antibodies

SARS-CoV-2 spike proteins were purchased from ACRObiosystems Inc. SARS-CoV-2 (Cov-19) S protein, His Tag, super stable trimer (MALS & NS-EM verified) (Cat. #SPN-C52H9) was used in early experiments to analyze IgG and IgM response as well as for Activated Immune Cell Marker assays (AIM). Subsequently, with the emergence of new variants of concern and increased availability of recombinant proteins, the following were purchased: SARS-CoV-2 UK Alpha S1 protein (HV69-70del, Y144del, N501Y, A570D, D614G, P681H, T716I, S982A, D1118H), His Tag (Cat. #SPN-C52H6); SARS-CoV-2 S UK Alpha protein RBD (N501Y), His Tag (Cat. #SPD-C52Hn); SARS-CoV-2 SA Beta S protein (L18F, D80A, D215G, 242-244del, R246I, K417N, E484K, N501Y, D614G, A701V) trimer 50ug #SPN-C52Hk; SARS-CoV-2 SA Beta S protein RBD (K417N, E484K, N501Y), His Tag (MALS verified) (Cat. #SPD-C52Hp); SARS-CoV-2 Brazil Gamma S1 protein (L18F, T20N, P26S, D138Y, R190S, K417T, E484K, N501Y, D614G, H655Y, T1027I, V11 (Cat. #SPN-C52Hg); SARS-CoV-2 India Delta spike S1 (T95I, G142D, E154K, L452R, E484Q, D614G, P681R), His Tag (Cat. # S1N-C52Ht); SARS-CoV-2 Omicron spike protein HRP (RBD, G339D, S371L, S373P, S375F, K417N, N440K, G446S, S477N, T478K, E484A, Q493R, G496S, Q498R, N501Y, Y505H, His Tag)-HRP (Cat# Z03730).

SARS-CoV-2 (COVID-19) spike antibody against the S1 and S2 subunits, were purchased from Genetex (Cat. #GTX135356 and #GTX632604) for western blot confirmation of S protein within EDV^{TM}. SARS-CoV-2 (2019-nCoV) spike RBD rabbit PAb, antigen affinity purified (Cat. #40592-T62, Sino Biological) was used for quantitation of the S protein within EDVs using ELISA.

Cell lines

JAWSII mouse bone marrow derived dendritic cells (ATCC® CRL-11904™) were grown in α-minimum essential medium (MEM; #M7145; Sigma) with ribonucleosides and deoxyribonucleosides (4 mM L-glut, 1 mM Sodium Pyruvate, 5 ng/ml GMCSF and 20% FBS) at 37°C, 5% CO_2.

Generation of plasmid expressing SARS-CoV-2 S protein under bacterial promoter

An expression cassette was generated by placing the coding nucleotide sequence for SARS-CoV-2 (Covid-19) spike protein (Wuhan sequence; GenBank MN908947.3) on the 3'-end of a modified β-lactamase promoter, which has been previously used for expression in *Salmonella typhimurium* strains [49]. The

expression cassette was then inserted between the KpnI 5' and SalI 3' sites of the M13 multiple cloning site of pUC57-Kan backbone plasmid to create pLac-CoV2. The sequence was optimised for *S. typhimurium* codon usage before manufacturing by Genscript services. A negative control plasmid, pLac-control, was created as above by removing the CoV2 sequence from the pLac-CoV2 (Fig. 1).

Cloning of pLac-CoV2 and pLac into Salmonella Typhimurium EDV producing strain and the assessment of plasmid and S protein within EDVs

Cloning

PLac-Cov2 and pLac-CoV2-control were electroporated into a chemically competent *S. typhimurium* intermediate strain, which lacks a plasmid restriction mechanism, using a Gene Pulser Xcell™ (Bio-Rad, Hercules CA) with settings 200 ohm, 25 Hz and 2.5 mV. Transformants were recovered in TSB medium for 1.5 h at 37°C before plating on TSB agar plates containing 75 µg/mL kanamycin (#K4000, Sigma-Aldrich, St. Louis, Missouri). Isolates were picked into TSB broth with 75 µg/mL kanamycin and plasmid DNA was extracted using the Qiagen miniprep kit as per manufacturer's instructions (#27104, Qiagen, Hilden, Germany). Subsequently, the extracted plasmid DNA from the 4004 strain was electroporated as above into the EnGeneIC Pty. Ltd. EDV^{TM} producing *S. typhimurium* strain (ENSm001). Clones containing pLac-CoV2 produce the encoded Covid-19 spike protein, which along with the plasmid DNA, becomes incorporated into EDVs during cell division to produce EDV-COVID. The EDVs containing pLac (EDV-CONTROL) were created in the same way to be used as a negative control.

To determine the plasmid content of EDV-COVID and EDV-CONTROL, plasmids were extracted from 2x10^9 EDVs using a Qiaprep Spin miniprep kit (Qiagen) following the manufacturer's instructions. Empty EDV were processed in the same manner as a control. The quantity of DNA plasmids was then measured by absorption at OD_{260nm} using a biophotometer (Eppendorf). The copy number of the plasmids were calculated using:

$$Number\ of\ copies = \frac{amount\ \times 6.22 \times 10^{23}}{length\ \times 10^{9} \times 660}$$

Western Blot

Proteins from 2 x 10^{10} EDV-COVID were extracted using 100 µL B-PER™ (Bacterial Protein Extraction Reagent; ThermoFisher) supplemented with 10% (v/v) lysozyme (Sigma-Aldrich) and 1% (v/v) DNase I (Cat. #EN0521, Qiagen). The extracted samples were then centrifuged at 12000 g for 10 min and the supernatant was collected. The pellet was also collected and resuspended in 100 µL PBS. 23 µL of the supernatant and pellet protein samples were co-incubated with 5 µL of loading buffer and 2 µL DTT (Sigma-Aldrich) at 80^{o}C for 20 min before the entire content of each sample was loaded onto a NuPAGE 4-12% Bis-Tris Mini Protein Gel (Cat. #NP0322BOX, ThermoFisher) and run at 190 V for ~80 min. The gel was then transferred using the iBlot 2 system (ThermoFisher) after which the membrane was blocked

using SuperBlock™ blocking buffer (Cat. #37515, ThermoFisher) and subsequently stained with 1:1000 Rabbit poly-clonal anti-SARS-CoV-2 spike (S1) antibody (Genetex) or 1:1000 mouse mono-clonal anti-SARS-CoV-2 spike (S2) antibody (Genetex) and incubated overnight at 4^{o}C. The membrane was then washed with PBST and incubated with HRP conjugated anti-rabbit (1:5000) (Abcam) or anti-mouse (1:5000) (ThermoFisher) IgG secondary antibody for 1 h at RT. The blot was developed using Lumi-Light Western Blot substrate (Cat. #12015200001**,** Roche) and visualized using a Chemidoc MP (Bio-Rad).

EDV S protein estimation by ELISA

4 x 10^{9} EDV-COVID particles were pelleted by centrifugation at 13000 g for 8 min. 100 µL of B-Per™ Bacteria lysis agent supplemented with 100 µg/reaction of lysozyme (Cat. #L6876, Sigma) and 5U/reaction rDNase I (Cat. #740963, Macherey-Nagel) was added to each sample and incubated on a vortex shaker for 2 h at 600 rpm at RT. The samples were then mixed with 1:5 Dithiothreitol (Cat. # 20290 ThermoFisher) and placed on an 80^{o}C heat block (Eppendorf) at 600 rpm agitation for a further 20 min. Protein quantity was assayed using the DC Protein Assay kit (Cat. #5000111, Bio-rad) following the manufacturer's specifications.

Standards were generated through serial dilution of the spike protein (ACRObiosystems) to achieve the following concentrations: 2000, 1000, 500, 250, 125, 62.5, 31.3 pg/mL. EDV-COVID S protein samples were diluted 1:1000 in PBS. Standards and EDV spike protein samples, were then coated on the ELISA plate, sealed, and incubated O/N at 4^{o}C. The plates were then washed 3 times with 300 µL PBST using a plate washer. 200 µL protein free blocking buffer (Cat. # 786-665; Astral Scientific) was added to the plate which was sealed and incubated at RT for 1 h.

Spike RBD Rabbit PAb detection antibody (Sino Biological) was diluted 1:10000 in 10 mL PBST and 100 µL per well was added and incubated for 1 h at RT. The plate was washed in PBST as above before addition of 100 µL sheep anti-rabbit IgG (H+L)-peroxidase (Cat. #SAB3700920; Merck, 1:10000) in 10 mL PBST. Sealed plates were incubated for 30 min at RT in the dark. The plate was washed again as above and 100 µL of TMB solution (Cat #34022; ThermoFisher) was added per well. The reaction was stopped by adding 50 µL of 2 M H_2SO_4 per well within minutes of TMB addition. The samples were analyzed at OD_{450nm} using a µQuant plate reader (Bio-TEK Instruments, Inc) and KC junior software.

Alpha-galactosylceramide loading into EDV-COVID

EDV-COVID nanoparticles carrying the S protein were purified in large batches through bio-fermentation of the parent bacteria *S. typhimurium*, followed by tangential flow filtration (TFF) to purify the EDV-COVID particles from the parent as previously described [9]. EDV-COVID particles were then buffer exchanged from media into PBS pH 7.4 (Dulbecco's; ThermoFisher) complemented with 0.5% tyloxapol (Cat. #T8761, Sigma-Aldrich) prior to loading with αGC based on a protocol described in Singh et al (2014) [50].

Alpha-galactosylceramide glycolipid adjuvant (αGC; Advanced Molecular Technologies, Melbourne) stocks were formulated in 100% DMSO (Sigma). Stock αGC was added to EDV-COVID solutions in PBS at

a final concentration of 10 μM (8.58 μg/mL equivalent). Co-incubation of EDV-COVID particles and αGC was performed at 37°C with mixing overnight. Unloaded αGC was removed by washing the particles in PBS pH 7.4 (Dulbecco's; ThermoFisher) through a 0.2 μm TFF system. EDV-COVID-αGC particles were then concentrated in PBS pH 7.4 followed by buffer exchange to 200 mM Trehalose (Cat. #T9531, Sigma) ready for vial filling and freeze-drying.

EDV-COVID-αGC batch vials underwent quality control testing including particle count, uniformity, sterility, S protein concentration, plasmid copy number and αGC concentration per 10^9 EDV particles, prior to use in animal experiments. Activity of loaded αGC through dendritic cell (DC) uptake and presentation through the CD1d T cell receptor was carried out as described below.

αGC uptake and presentation by murine DCs

JAWSII cells (ATCC) were treated with EDV-COVID-αGC in a 96-well Perfecta3D hanging drop plate (Cat. #HDP1385, Sigma-Aldrich) at $1x10^9$ EDV-COVID-αGC per cell. JAWSII cells treated with 2 μg/mL αGC (Advanced Molecular Technologies) served as a positive control. The cultures were then incubated for 24 h at 37^{o}C with 5% CO_2 and cells were collected and stained with a PE conjugated CD1d: αGC complex antibody (Cat. # **12-2019-82**, ThermoFisher, 1:2000) and analyzed using a Gallios flow cytometer (Beckman). The results were analyzed using Kaluza Analysis software (V.2.1, Beckman).

Detection of spike protein and CD1d associated αGC in murine DCs following EDV-COVID-αGC co-incubation

JAWSII cells (ATCC) were seeded onto a 96 well hanging drop plate (Sigma-Aldrich) at 5×10^4 cells/well. EDV only, EDV-αGC, EDV-CONTROL, EDV-COVID and EDV-COVID-αGC were co-incubated with the cells at $1x10^9$ EDVs per well. Untreated JAWSII cells were used as controls. The samples were cultured at 37^{o}C with 5% CO_2 for 48 h before collected and co-stained with PE anti-mouse αGC:CD1d complex antibody (ThermoFisher, 1:2000) and SARS-CoV-2 S1 protein polyclonal primary antibody (Genetex, 1:2000) at room temperature for 30 min in the dark. The samples were then stained with Alexa Fluor 647 goat anti-rabbit IgG (H+L) highly cross-adsorbed secondary antibody (ThermoFisher, 1:1000) at 4^{o}C for a further 20 min and analysed using a Gallios flow cytometer (Beckman Coulter). Mouse IgG2a and rabbit IgG (Biolegend) were used as isotype controls. DAPI was used to differentiate live/dead cells and single stained samples were used to generate compensation. The samples were analysed using the Kaluza analysis software (V2.1, Beckman Coulter).

Extraction of αGC from EDV-COVID-αGC for quantitation

An αGC extraction method was adapted from previous similar studies [51, 52]. The necessary number of EDV vials were taken to achieve a total of 4×10^{10} EDVs per sample for extraction of αGC. An EDV only sample was used as a negative control.

All lyophilized vials were resuspended in 400 µL of PBS (Dulbecco's Ca^{2+} Mg^{2+} free, ThermoFisher). Each sample was aliquoted to give ~2 x 10^{10} EDVs per sample in Eppendorf tubes (i.e., two tubes per sample) and all samples were centrifuged @ 13200 rpm for 7.5 min. The supernatant was removed from each sample and the EDV pellets were resuspended in 800 µL PBS for each 2 x 10^{10} and centrifuged again as above. The supernatant was removed once again, and all samples were resuspended in 500 µL of UltraPure™ H_2O (Cat. # 10977015, ThermoFisher).

For α-GC extraction, each 500 µL sample was transferred to a conical bottom 2 mL microtube (Axygen). One stainless steel bead (5 mm) was added to each sample and samples were then homogenized using agitation on the Qiagen TissueLyser II homogeniser (Qiagen). Homogenisation was carried out in two rounds of 2 min agitations at 25 Hz with a brief stoppage between sets. Lysates were then removed to fresh tubes combining 500 µL aliquots from each sample to give a 1 mL sample (leaving the bead behind).

Each 1mL sample was then extracted for lipids by adding 1 mL of chloroform/methanol (2:1 CHCl3: MeOH ratio), shaking vigorously by hand and incubating at 37°C for 15 min with sonication every 5 min for 1 min. Following 15 min, samples were centrifuged at 2000 g for 10 min in a benchtop micro centrifuge. The organic layer (bottom) was removed to a fresh tube. The samples were then dried before analysis.

Quantitative LC-MS/MS Analysis of αGC

The standard, α-galactosylceramide (αGC), and the internal standard (IS), D-galactosyl-ß-1,1' N-palmitoyl-D-erythro-sphingosine were dissolved in DMSO to 1 mM or 2 mM with heating at 60-80°C for 5 min if necessary to dissolve. Prior to data acquisition the standard stock solution was used to prepare stock dilutions in MEOH:$H_2$0 (95:5). A working IS dilution was prepared with final concentration of 200 ng/mL.

Standards were prepared by using five calibration points of αGC (STD) (62.5, 125, 250, 500, and 1 000 ng/mL) spiked with 200 ng/mL IS [52]. The standard: IS area ratios were used as calibration curve (CC) points or linearity against which the unknown samples were quantified. The samples were dried and reconstituted in 1ml of working IS dilution.

Samples were acquired along with the freshly prepared CC standards on a TSQ Altis (ThermoFisher) triple quadruple mass spectrometer (MS) interfaced with Vanquish (ThermoFisher) UHPLC (Ultra High-Performance Liquid Chromatography) (LC). The LC-MS instrument method employed for data acquisition was optimised as per Sartorius et. al. (2017) [52]. Xcalibur and TraceFinder software were used for data acquisition and analysis respectively (ThermoFisher).

The chromatographic analysis (LC) was performed on an Acquity BEH Phenyl column (Waters, 100 × 2.1 mm, 1.7 µm), eluted with a short gradient program from 95:5 MeOH/H2O to 100% MeOH in 1 min followed by an isocratic elution at 100% MeOH for 4 min. Flow rate was set at 0.4 mL/min and column temperature at 40°C. αGC eluted at a RT of 1.53 min, IS at 1.07 min. Two MRM transitions were

monitored for both STD and IS for quantitative purposes and to confirm analytical identification. The most intense transitions for each compound (i.e., m/z 856.7 > 178.9 for STD and m/z 698.5 > 89.2 for IS) were used as analytical responses.

Animal studies

Female BALB/C mice, 6-8 weeks old were obtained from the Animal Resource Centre in Western Australia. The mice were acclimatized for one week before the experiments commenced. All experiments were subject to assessment and approval by the EnGeneIC Animal Ethics Committee according to the "Australian code for the use and care of animals for scientific purposes". Treatment groups (n = 4-10 depending on experiment) included EDV-COVID-αGC as well as control groups consisting of saline, EDV, EDV-αGC, EDV-CONTROL (Control Plasmid) and EDV-COVID. Initial experiments involved a 2 x 10^9 i.m. particle dose into a single flank at day 0, followed by a booster of 1 x 10^9 at day 21. Subsequent experiments applied a higher i.m. only dose of 3 x 10^9 particles split into 1.5 x 10^9 per back flank due to limitations of particle volume/concentration acceptable per flank, with a boost of the same dose and mode of delivery at day 21. Depending on the experiment, serum and tissues were collected at 8 h, day 7, day 21 and day 28 post-initial injection. Blood was collected via heart puncture immediately following euthanasia, or tail bleeding for ongoing analysis. Other tissues harvested include spleen, lymph nodes, and bone marrow from the femur.

Isolation of Serum

Whole blood samples in SST vacutainers (Cat. #455092, VACUETTE®) were allowed to clot at RT for 1 h. After centrifugation for 10 min at 800 g the serum layer was aliquoted and stored at -80°C for SARS-CoV-2 specific antibody detection by ELISA and neutralizing antibody assays.

Splenocyte isolation

Tissue suspensions were isolated from dissected spleens of treated BALB/C mice using a Dounce homogenizer and resuspended in RPMI-1640 medium (Cat. #R8758, Sigma-Aldrich,). The homogenized tissue was then filtered through sterile 70 µm MACS SmartStrainers (Cat. #130-110-916, Miltenyi Biotec) and incubated with Red Cell Lysing Buffer Hybri-Max™ (Cat. #R7757, Sigma-Aldrich) as recommended by the manufacturer. Cells were then resuspended in 2.5 mL of autoMACS running buffer (Cat. #130-091-221, Miltenyi Biotec) and passed through a 70 µm MACS SmartStrainer to obtain a single-cell suspension.

Cytokine ELISA

IFNγ, TNFα, IL-6, IFNα, IL-12p40, IL-10, IL-2 and IL-4 from mouse sera were measured using DuoSet® ELISA kits from R&D Systems according to manufacturer's instructions (Table S2). Serum levels of IL-21 was analyzed using a LEGEND MAX Mouse IL-21 ELISA kit (Biolegend) following the manufacturer's

instructions. Cytokine concentration was determined by calculating absorbance of the samples against standard curves constructed within the same assay using purified material.

S-protein RBD and S1 IgG/IgM serum titer ELISA

For analysis of anti-RBD specific IgG and IgM antibodies, 96-well plates (Immulon 4 HBX; Thermo Fisher Scientific) were coated at 4°C with 50 µL per well of a 2 µg/mL solution of RBD or S1 protein of the corresponding variant being tested (ACRObiosystems) suspended in PBS (GIBCO). On the following day, the coating protein solution was removed and 100 µL of 3% skim milk blocking solution in PBS/0.1% Tween 20 (PBST) or protein free blocking solution (G-Biosciences) was added and incubated at RT for 1 h. Serial dilutions of mouse serum were prepared in 1% skim milk/PBST or protein free blocking solution. The blocking solution was removed and 100 µL of each serum sample was added to the plates and incubated for 2 h at RT. Following incubation, the wells were washed three times with 250 µL of 0.1% PBST, before adding 100 µL of goat anti-mouse IgG (H+L) or IgM (Heavy)–horseradish peroxidase (HRP) conjugated secondary antibody (Cat # 31430, #62-6820; ThermoFisher, 1:3000) prepared in 0.1% PBST. The samples were incubated at RT for 1 h and washed three times with 0.1% PBST. Once completely dry, the samples were visualized by incubating with TMB. The reactions were then terminated, and the samples were read at OD_{490nm} using a KC Junior plate reader (BioTek Instruments).

Antibody titer was determined using ELISA by generating 1:3 serial dilution of the treated mouse serum samples and is expressed as the inverse of the highest dilution with a positive result.

B cell extraction from murine bone marrow

0.5 mL microfuge tubes were punctured at the base with a 21-gauge needle and placed inside a 2 mL tube. The isolated murine tibia and femur were placed in the 1 mL tubes with the cut side of the bone at the bottom. Bone marrow cells were extracted from the tibia and femur via 30 s centrifugation at ≥10000 g. Pelleted cells were resuspended in 1 mL RPMI-1640 medium (Cat. #R8758, Sigma-Aldrich) and incubated with Hybri-Max™ Red Cell Lysing Buffer (Cat. #R7757, Sigma-Aldrich) for 5 min. The lysis buffer was neutralized with 15 mL of RPMI-1640 medium supplemented with 10% Fetal Bovine Serum (FBS) (Cat. #AUFBS, Interpath) and centrifuged at 300 g for10 min. Cells were resuspended in a final volume of 10 mL of RPMI-1640 medium for final counting. B cells were isolated using the Pan B Cell Isolation Kit (Cat. #130-095-813, Miltenyi Biotec) as per manufacturers' instructions.

B cell stimulation and ELISA

ELISA micro plates were coated with 2 µg/mL SARS-CoV-2 spike protein trimer (ACRObiosystems) and incubated overnight at 4°C. Microplates were washed 3x with phosphate-buffered saline (PBS) and blocked with 200 µl/well of Protein-Free Blocking Buffer PBST (Cat. #786-665, G-Biosciences) for 2 h at RT.

Mouse splenocytes were isolated from treated mice and $1x10^5$ cells were seeded into each well in 200 µL AIMV media and incubated at 37°C for 48 h.

At the end of the incubation period, the cells were removed from each well and each microplate was washed 5x with 200 µL/well of 0.05% Tween 20 in PBST. The samples were then incubated in 100 µL/well of 1:5000 mouse IgG-HRP in PBST for 2 h at RT in the dark before washing 3x in 250 µL PBST. The presence of Covid specific IgG was detected by adding 100 µL/well of TMB Substrate System and allowed to incubate up to 20 min or until color solution formed. Enzyme reaction was stopped by adding 50 µL/well of 2N H2SO4 Stop Solution. The samples were analyzed using a CLARIOstar microplate reader (BMG LABTECH) at OD_{450nm} with OD_{540nm} as the reference wavelength and analyzed using the MARS software.

Activation-Induced Markers (AIM) Assay

Isolated spleen cells were seeded at 1 x 10^6 cells/200 µL/well in AIMV (Life Technologies) serum free media in a 96-well U-bottom plate. Cells were stimulated with 1 µg/mL SARS-CoV-2 trimer (ACRObiosystems) for 24 h at 37°C, 5% CO_2. 1 µg/mL DMSO was used as a negative control and 10 µg/mL PHA (Cat. # L2769-2MG; Sigma) as a positive control. After 24 h of stimulation, samples were collected in 1.5 mL microfuge tubes by pipetting up and down to collect the cells and centrifuged at 300 g for 10 min. The supernatant was collected and frozen for processing for IFNγ by ELISA (DuoSet, R&D Systems).

For T-cell activation staining the cell pellets from above were washed twice in 500 µL FACS buffer, centrifuging as above. Final cell pellets were resuspended in 500 µL FACS buffer and stained with the appropriate antibody (included in the kit) for 30 min at RT in the dark (Table S3). Cells were then centrifuged at 300 g for 5 min and washed twice with 500 µL FACS buffer. Cells were then fixed in 1% paraformaldehyde for 10 min at 4°C and after that centrifuged at 300 g for 5 min again. Final resuspension was in 300 µL of FACS buffer before analyzing on a Gallios flow cytometer (Beckman). Single stain samples and mouse IgG isotype controls were used to create compensation for the staining.

Th1/Th2 Phenotyping

Th1/Th2 phenotyping was carried using the Mouse Th1/Th2/Th17 phenotyping kit (Cat. #560758, BD). Firstly, as per AIM assay, isolated spleen cells were seeded at 1 x 10^6 cells/200 µL/ well in AIMV (Life Technologies) serum free media in a 96-well U-bottom plate. Cells were stimulated with 1 µg/mL SARS-CoV-2 trimer (ACRObiosystems) for 24 h at 37°C, 5% CO_2. 1 µg/mL DMSO was used as a negative control. After 24 h of stimulation, 1 µL of BD GolgiStop™ (protein transport inhibitor, Cat. #51-2092KZ; BD) per 200 µL /well of cell culture was added, mixed thoroughly, and incubated for a further 2 h at 37°C. Cells were then centrifuged at 250 g for 10 min and washed 2 times with stain buffer (FBS) (Cat# 554656; BD). The cells were counted and approximately 1 million cells were transferred to each flow test tube for immunofluorescent staining as per manufacturer's instructions. Cells were protected from light

throughout the staining procedure. Firstly, cells were fixed by spinning at 250 g for 10 min at RT and thoroughly resuspending in 1 mL of cold BD Cytofix™ buffer (provided in the kit or Cat# 554655; BD) and incubated for 10-20 min at RT. Following fixation cells were pelleted at 250 g for 10 min at RT and washed twice at RT in stain buffer (FBS). The stain buffer was removed by spinning and the cell pellet was resuspended in 1X BD Perm/Wash™ buffer (Cat# 554723, BD) diluted in distilled water, and incubated at RT for 15 min. Cells were spun down at 250 g for 10 min at RT and the supernatant removed. For staining, the fixed/permeabilized cells were thoroughly resuspended in 50 µL of BD Perm/Wash™ buffer incubated with 20 µL/tube of cocktail included in the kit (Mouse CD4 PerCP-Cy5.5 (clone: RM4-5), Mouse IL-17A PE (clone: TC11-18H10.1), Mouse IFN-GMA FITC (clone: XMG1.2), Mouse IL-4 APC (clone: 11B11) or appropriate negative control. Samples were incubated at RT for 30 min in the dark before proceeding to FACs analysis on a Gallios flow cytometer (Beckman). Compensation was performed manually for each channel using single stained controls.

SARS-Cov-2 Surrogate Virus Neutralization Test (Mouse and Human samples)

Assessment of neutralizing antibodies was carried out using the FDA approved “cPASS SARS-Cov-2 Surrogate Virus Neutralization Test Kit” (Cat. # L00847-A; Genscript) [14]. The kit is a blocking ELISA detection tool mimicking the virus neutralization process, suitable for use with serum from mice and other species. The capture plate is precoated with hACE2 protein. The necessary of hACE2 coated plate strips were placed on the plate and the remainder stored at 2-8 °C. HRP-RBD (Wuhan, Genscript) was diluted 1:1000 in HRP dilution buffer provided to a total of 10 mL as per protocol. Mouse and human serum samples, PBMC supernatant and positive and negative controls were diluted 1:10 (10 µL + 90 µL sample dilution buffer) and pre-incubated with HRP-RBD in a 1:1 ratio (60 µL + 60 µL) to allow binding of neutralizing Abs with HRP-RBD. Mixes were incubated at 37°C for 30 min. 100 µL of samples or controls were added to the appropriate wells. The plate was covered with plate sealer and incubated at 37°C for 15 min. The sealer was then removed and the plate washed 4 times with 260 µL of 1X wash solution. The plate was pat dried after washing. 100 µL of TMB solution was then added to each well and the plate incubated in the dark at RT for up to 15 min. 50 µL of stop solution was added to terminate the reactions. Absorbance was analyzed at OD_{450nm} immediately using a CLARIOstar microplate reader. HACE2 receptor binding inhibition was calculated using the formula provided by the manufacturer (% inhibition=1-(OD value of sample/OD value of negative control) x 100%. As per spec sheet a positive value was interpreted as > 30% and a negative as < 30%.

For the assessment of neutralizing antibodies against variant SARS-CoV-2 strains the following HRP-RBD proteins were purchased from Genscript for substitution into the cPASS kit: SARS-CoV-2 Alpha spike protein (RBD, E484K, K417N, N501Y, Avi & His tag)-HRP (Cat. #Z03596), SARS-CoV-2 Beta spike protein (RBD, N501Y, Avi & His tag)-HRP (Cat. #Z03595), SARS-CoV-2 Gamma spike protein (RBD, E484K, K417T, N501Y, Avi & His Tag)-HRP (Cat. #Z03601), SARS-CoV-2 Delta spike protein (RBD, L452R, T478K, Avi & His Tag)-HRP (Cat. #Z03614), SARS-CoV-2 Omicron spike protein HRP (RBD, G339D, S371L, S373P, S375F, K417N, N440K, G446S, S477N, T478K, E484A, Q493R, G496S, Q498R, N501Y, Y505H, His Tag)-HRP (Cat# Z03730).

Neutralizing titer analysis

Serum samples were diluted in 1:1, 1:10, 1:20, 1:40, 1:80, 1:160, 1:320 and 1:640, and analyzed using the FDA approved “cPASS SARS-Cov-2 Surrogate Virus Neutralization Test Kit” against the wildtype SARS-CoV-2 virus as described previously. The neutralizing titer was determined as the final serum dilution from which resulted in a RBD to hACE2 binding inhibition of greater or equal than 30%.

Statistical analysis

Student’s T-tests and Ordinary one-way ANOVA with Brown-Forsythe test and Bartlett’s test were conducted using Prism 8 (GraphPad). A p value of <0.05 is statistically significant.

Pancreatic Cancer Clinical Trial Data

All participants in clinical trials conducted at Frankston Private Hospital and Sydney Adventist Hospital signed a patient informed consent form prior to commencement of treatment. Ethics approval granted by Bellberry Limited Human Research Ethics Committee D (00444). Clinical Data presented in this publication is from Clinical Trial ACTRN12619000385145, a Phase I/IIa study of EGFR-Targeted EDV^{TM} carrying the cytotoxic drug PNU-159682 (E-EDV-682) with concurrent immunomodulatory adjuvant non-targeted EDVs carrying an immunomodulator (EDV-αGC) in (i) Cohort 1, subjects with advanced pancreatic cancer solid tumors who have no curative treatment options and (ii) Cohort 2, with other EGFR-expressing solid tumors who failed first or second line therapies or where standard therapies are not appropriate. The results were presented as mean of all 13 patients’ values $\pm$ SEM.

Human subjects

Individuals provided informed consent and were enrolled in the study (https://www.anzctr.org.au/Trial/Registration/TrialReview.aspx?id=382580&isReview=true) with approval from St. Vincent’s Hospital Melbourne Human Research Ethics Committee. All participants were otherwise healthy and did not report any history of chronic health conditions. Subjects were identified as SARS-CoV-2 naive via PCR test and naïve for prior COVID-19 vaccines. All subjects received a dose of 8×10^9 EDV-COVID-αGC with an equal booster dose at day 21. Samples were collected at 4 time points: pre-vaccine baseline (time point 1), day 21 before the booster vaccination (time point 2), and day 28 one week post-boost (time point 4). Subjects are also scheduled to return for a 3 month and 6 month time point. Each study visit included collection of 20 mL of peripheral blood. The study began in September 2021 and at time of submission there are a number of volunteers that have come forward to be part of the study. Full data (all time points) at this time is available for four volunteers.

FACS analysis of T cells and B cells in Human Samples

T cell analysis was conducted using DuraClone IM T cell subsets tube (Cat # B53328, Beckman Coulter). 1×10^6 purified PBMCs were added to the tubes directly in 100µL and incubated at RT for 30 min in the dark. The samples were then pelleted at 300g for 5min and washed once in 3mL of PBS. The final

samples were resuspended in 500µL of PBS with 0.1% formaldehyde. The compensation for the assay was generated using the Compensation Kit provided in the IM DuraClone T cell subset tube using purified PBMCs.

B cell analysis was conducted using DuraClone IM B cells tube (Cat # B53318, Beckman Coulter). 1 x 10^6 purified PBMCs were added to the tubes directly in 100µL and incubated at RT for 30 min in the dark. The samples were then pelleted at 300g for 5min and washed once in 3mL of PBS. The final samples were resuspended in 500µL of PBS with 0.1% formaldehyde. The compensation for the assay was generated using the Compensation Kit provided in the IM DuraClone B cell subset tube using purified PBMCs.

Samples were processed using a Gallios flow cytometer (Beckman) and the results were analyzed using the Kaluza Analysis software (ver 2.1, Beckman).

Activation-Induced Markers (AIM) Assay in Human samples

Volunteer PBMCs were seeded at 1 x 10^6 cells/200 µL/well in AIMV (Life Technologies) serum free media in a 96-well U-bottom plate. Cells were stimulated with 2 µg/mL SARS-CoV-2 trimer (ACRObiosystems) for 24 h at 37^{o}C, 5% CO_2. 2 µg/mL DMSO was used as a negative control and PHA (Cat. # 00-49-03; eBiosciences) as a positive control. After 24 h of stimulation, samples were collected in 1.5 mL microfuge tubes by pipetting up and down to collect the cells and centrifuged at 300 g for 10 min. The supernatant was collected and frozen for processing for IFNγ by ELISA (DuoSet, R&D Systems) and for SARS-CoV-2 wildtype surrogate virus neutralization test using the cPASS kit (Genscript). The negative controls of the samples were also used for IL-21 analysis using IL-21 Human ELISA kit (Cat #: BMS2043, ThermoFisher) following the manufacturer's instructions.

Declarations

Acknowledgements:

The authors thank the following members of the EnGeneIC team: EDV manufacturing; Richard Paulin, Arash Pedram, Vatsala Brahmbhatt, Timothy Morgan and Cathy Creely. EDV QA/QC; Scott Pattison, Anna Pogudin, Kunal Kalra.

Funding: This project was fully funded by EnGeneIC Pty Ltd.

Author contributions:

H.B., J.A.M. conceptualized the study. H.B., J.A.M., S.Y.G., N.B.A-M. designed the study. S.Y.G., N.B.A-M. supervised all the experiments. S.Y.G., N.B.A-M., J.M-W., N.P., N.V. performed the experiments and collated all the data. J.M-W. led and supervised mouse experiments. B.W. helped with discussions and critical review of the manuscript. V.G. and G.M. were the principal investigator and co-investigator respectively in the Carolyn Clinical trial. H.B., J.A.M., S.Y.G., and N.B.A-M. wrote the manuscript with input from all the authors.

Competing interests:

H.B., J.A.M., N.B.A-M., J.M-W. and B.R.G.W. are shareholders in EnGeneIC Ltd. H.B., J.A.M., and B.R.G.W. are on the Board of EnGeneIC Ltd.

Data and materials availability:

All data needed to evaluate the conclusions in the paper are present in the paper or the supplementary materials.

Supplementary Materials:

Materials and Methods

Fig. S1-S3

Tables S1 to S3

References (*1–49*)

References

1. Chan, J.F. et al. Genomic characterization of the 2019 novel human-pathogenic coronavirus isolated from a patient with atypical pneumonia after visiting Wuhan. *Emerging microbes & infections* **9**, 221-236 (2020).

2. Song, W., Gui, M., Wang, X. & Xiang, Y. Cryo-EM structure of the SARS coronavirus spike glycoprotein in complex with its host cell receptor ACE2. *PLoS pathogens* **14**, e1007236 (2018).

3. Lan, J. et al. Structure of the SARS-CoV-2 spike receptor-binding domain bound to the ACE2 receptor. *Nature* **581**, 215-220 (2020).

4. Brouwer, P.J.M. et al. Potent neutralizing antibodies from COVID-19 patients define multiple targets of vulnerability. *Science (New York, N.Y.)* **369**, 643-650 (2020).

5. Liang, W. et al. Cancer patients in SARS-CoV-2 infection: a nationwide analysis in China. *Lancet Oncol* **21**, 335-337 (2020).

6. Haidar, G. et al. Immunogenicity of COVID-19 Vaccination in Immunocompromised Patients: An Observational, Prospective Cohort Study Interim Analysis. *medRxiv*, 2021.2006.2028.21259576 (2021).

7. Uriu, K. et al. Ineffective neutralization of the SARS-CoV-2 Mu variant by convalescent and vaccine sera. *bioRxiv*, 2021.2009.2006.459005 (2021).

8. Pegu, A. et al. Durability of mRNA-1273 vaccine-induced antibodies against SARS-CoV-2 variants. *Science (New York, N.Y.)* **373**, 1372-1377 (2021).

9. MacDiarmid, J.A. et al. Bacterially derived 400 nm particles for encapsulation and cancer cell targeting of chemotherapeutics. *Cancer Cell* **11**, 431-445 (2007).

10. MacDiarmid, J.A. et al. Sequential treatment of drug-resistant tumors with targeted minicells containing siRNA or a cytotoxic drug. *Nat Biotechnol* **27**, 643-651 (2009).

11. Kao, S.C. et al. A Significant Metabolic and Radiological Response after a Novel Targeted MicroRNA-based Treatment Approach in Malignant Pleural Mesothelioma. *Am J Respir Crit Care Med* **191**, 1467-1469 (2015).

12. van Zandwijk, N. et al. Safety and activity of microRNA-loaded minicells in patients with recurrent malignant pleural mesothelioma: a first-in-man, phase 1, open-label, dose-escalation study. *Lancet Oncol* **18**, 1386-1396 (2017).

13. Whittle, J.R. et al. First in human nanotechnology doxorubicin delivery system to target epidermal growth factor receptors in recurrent glioblastoma. *J Clin Neurosci* **22**, 1889-1894 (2015).

14. Tan, C.W. et al. A SARS-CoV-2 surrogate virus neutralization test based on antibody-mediated blockage of ACE2-spike protein-protein interaction. *Nat Biotechnol* **38**, 1073-1078 (2020).

15. Jung, J., Rajapakshe, D., Julien, C. & Devaraj, S. Analytical and clinical performance of cPass neutralizing antibodies assay. *Clinical biochemistry* (2021).

16. Waschbisch, A. et al. Analysis of CD4+ CD8+ double-positive T cells in blood, cerebrospinal fluid and multiple sclerosis lesions. *Clinical and experimental immunology* **177**, 404-411 (2014).

17. Huang, Q., Hu, J., Tang, J., Xu, L. & Ye, L. Molecular Basis of the Differentiation and Function of Virus Specific Follicular Helper CD4+ T Cells. *Frontiers in Immunology* **10** (2019).

18. Bricard, G. & Porcelli, S.A. Antigen presentation by CD1 molecules and the generation of lipid-specific T cell immunity. *Cellular and molecular life sciences : CMLS* **64**, 1824-1840 (2007).

19. Bergamaschi, C. et al. Systemic IL-15, IFN-γ, and IP-10/CXCL10 signature associated with effective immune response to SARS-CoV-2 in BNT162b2 mRNA vaccine recipients. *Cell reports* **36**, 109504 (2021).

20. Sagnella, S.M. et al. Cyto-Immuno-Therapy for Cancer: A Pathway Elicited by Tumor-Targeted, Cytotoxic Drug-Packaged Bacterially Derived Nanocells. *Cancer Cell* **37**, 354-370 e357 (2020).

21. Hermans, I.F. et al. NKT cells enhance CD4+ and CD8+ T cell responses to soluble antigen in vivo through direct interaction with dendritic cells. *Journal of immunology (Baltimore, Md. : 1950)* **171**, 5140-

5147 (2003).

22. Vinuesa, C.G., Linterman, M.A., Yu, D. & MacLennan, I.C. Follicular Helper T Cells. *Annual review of immunology* **34**, 335-368 (2016).

23. Sattler, A. et al. SARS-CoV-2-specific T cell responses and correlations with COVID-19 patient predisposition. *J Clin Invest* **130**, 6477-6489 (2020).

24. Eertwegh, A. et al. In vivo CD40-gp39 interactions are essential for thymus-dependent humoral immunity. I. In vivo expression of CD40 ligand, cytokines, and antibody production delineates sites of cognate T-B cell interactions. *The Journal of experimental medicine* **178**, 1555-1565 (1993).

25. Toellner, K.M., Gulbranson-Judge, A., Taylor, D.R., Sze, D.M. & MacLennan, I.C. Immunoglobulin switch transcript production in vivo related to the site and time of antigen-specific B cell activation. *Journal of Experimental Medicine* **183**, 2303-2312 (1996).

26. Garside, P. et al. Visualization of specific B and T lymphocyte interactions in the lymph node. *Science (New York, N.Y.)* **281**, 96-99 (1998).

27. Ma, C.S. & Deenick, E.K. Human T follicular helper (Tfh) cells and disease. *Immunology and cell biology* **92**, 64-71 (2014).

28. Beier, K.C. et al. Induction, binding specificity and function of human ICOS. *European journal of immunology* **30**, 3707-3717 (2000).

29. Hu, H. et al. Noncanonical NF-kappaB regulates inducible costimulator (ICOS) ligand expression and T follicular helper cell development. *Proc Natl Acad Sci U S A* **108**, 12827-12832 (2011).

30. Bonhagen, K. et al. ICOS+ Th cells produce distinct cytokines in different mucosal immune responses. *European journal of immunology* **33**, 392-401 (2003).

31. Löhning, M. et al. Expression of ICOS in vivo defines CD4+ effector T cells with high inflammatory potential and a strong bias for secretion of interleukin 10. *J Exp Med* **197**, 181-193 (2003).

32. Bauquet, A.T. et al. The costimulatory molecule ICOS regulates the expression of c-Maf and IL-21 in the development of follicular T helper cells and TH-17 cells. *Nature immunology* **10**, 167-175 (2009).

33. Crotty, S. T follicular helper cell differentiation, function, and roles in disease. *Immunity* **41**, 529-542 (2014).

34. Avery, D.T., Bryant, V.L., Ma, C.S., de Waal Malefyt, R. & Tangye, S.G. IL-21-induced isotype switching to IgG and IgA by human naive B cells is differentially regulated by IL-4. *Journal of immunology (Baltimore, Md. : 1950)* **181**, 1767-1779 (2008).

35. Avery, D.T. et al. B cell-intrinsic signaling through IL-21 receptor and STAT3 is required for establishing long-lived antibody responses in humans. *J Exp Med* **207**, 155-171 (2010).

36. MacLennan, I.C. et al. Extrafollicular antibody responses. *Immunological reviews* **194**, 8-18 (2003).

37. Jacob, J., Kelsoe, G., Rajewsky, K. & Weiss, U. Intraclonal generation of antibody mutants in germinal centres. *Nature* **354**, 389-392 (1991).

38. MacLennan, I.C. Germinal centers. *Annual review of immunology* **12**, 117-139 (1994).

39. Gunn, M.D. et al. A B-cell-homing chemokine made in lymphoid follicles activates Burkitt's lymphoma receptor-1. *Nature* **391**, 799-803 (1998).

40. Ansel, K.M., McHeyzer-Williams, L.J., Ngo, V.N., McHeyzer-Williams, M.G. & Cyster, J.G. In vivo-activated CD4 T cells upregulate CXC chemokine receptor 5 and reprogram their response to lymphoid chemokines. *J Exp Med* **190**, 1123-1134 (1999).

41. Schaerli, P. et al. CXC chemokine receptor 5 expression defines follicular homing T cells with B cell helper function. *J Exp Med* **192**, 1553-1562 (2000).

42. Kim, C.H. et al. Subspecialization of CXCR5+ T cells: B helper activity is focused in a germinal center-localized subset of CXCR5+ T cells. *J Exp Med* **193**, 1373-1381 (2001).

43. Breitfeld, D. et al. Follicular B helper T cells express CXC chemokine receptor 5, localize to B cell follicles, and support immunoglobulin production. *J Exp Med* **192**, 1545-1552 (2000).

44. Pène, J. et al. Cutting edge: IL-21 is a switch factor for the production of IgG1 and IgG3 by human B cells. *Journal of immunology (Baltimore, Md. : 1950)* **172**, 5154-5157 (2004).

45. https://covid19.who.int/ (2021).

46. Cele, S. et al. Escape of SARS-CoV-2 501Y.V2 from neutralization by convalescent plasma. *Nature* **593**, 142-146 (2021).

47. Tan, L. et al. Lymphopenia predicts disease severity of COVID-19: a descriptive and predictive study. *Signal Transduction and Targeted Therapy* **5**, 33 (2020).

48. Ewer, K.J. et al. T cell and antibody responses induced by a single dose of ChAdOx1 nCoV-19 (AZD1222) vaccine in a phase 1/2 clinical trial. *Nature Medicine* **27**, 270-278 (2021).

49. Su, G.F., Brahmbhatt, H.N., Wehland, J., Rohde, M. & Timmis, K.N. Construction of stable LamB-Shiga toxin B subunit hybrids: analysis of expression in Salmonella typhimurium aroA strains and stimulation of B subunit-specific mucosal and serum antibody responses. *Infection and immunity* **60**, 3345-3359 (1992).

50. Singh, M. et al. Direct incorporation of the NKT-cell activator alpha-galactosylceramide into a recombinant Listeria monocytogenes improves breast cancer vaccine efficacy. *Br J Cancer* **111**, 1945-1954 (2014).

51. von Gerichten, J. et al. Diastereomer-specific quantification of bioactive hexosylceramides from bacteria and mammals. *J Lipid Res* **58**, 1247-1258 (2017).

52. Sartorius, R. et al. Vectorized Delivery of Alpha-GalactosylCeramide and Tumor Antigen on Filamentous Bacteriophage fd Induces Protective Immunity by Enhancing Tumor-Specific T Cell Response. *Front Immunol* **9**, 1496 (2018).

Figures

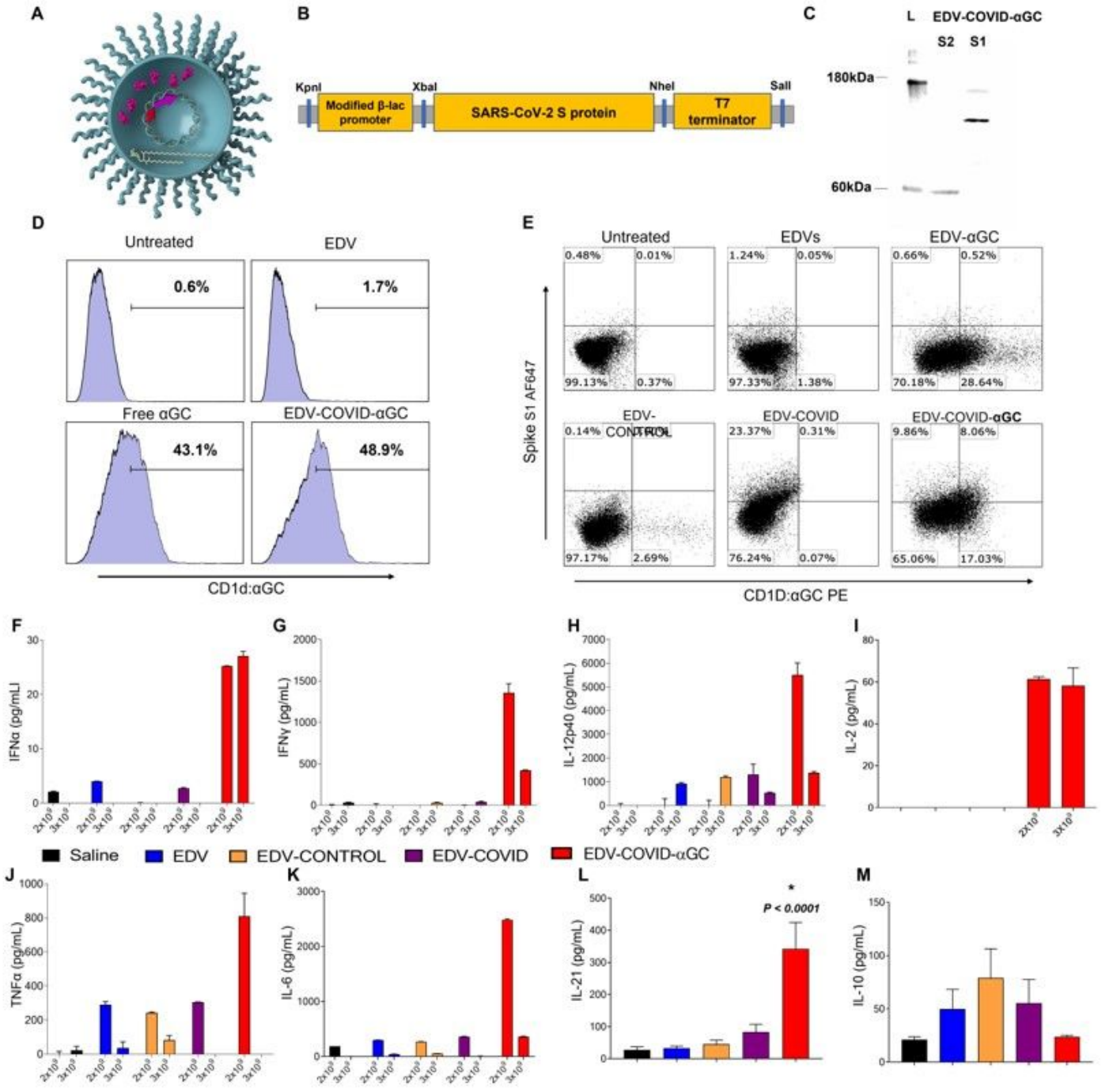

Figure 1

SARS-CoV-2 S-protein construct design, antigen processing and presentation to DC cells and ability to elicit Th1 and Th2 responses. (**A**) Image of EDV-COVID-αGC depicting the LPS, membrane and nanocell contents including plac-CoV-2 plasmid, S-protein and αGC. (**B**) Construct: SARS-CoV-2 spike protein nucleotide sequence (Genbank MN908947.3) at the 3'-end of a modified constitutive gene expression β-lactamase promoter and inserted between KpnI 5' and SalI 3' sites of the M13 multiple cloning site of PUC57-Kan backbone plasmid to create plac-CoV2. (**C**) Western blot analysis using MAbs against the S1 and S2 subunit demonstrated the presence of the S-protein within EDV-COVID-αGC. (**D**) FACS analysis showing that EDV-COVID-αGC was able to effectively deliver αGC into murine bone marrow derived,

JAWSII, cells and presented through CD1d-ligand to a similar efficiency as free αGC. (**E**) Co-staining of JAWSII cells with anti-CD1d:αGC and anti-spike Abs demonstrating αGC and S-protein delivery by EDVs with EDV-COVID-αGC delivering both S-protein and αGC on the same cell surface. (**F-H**) I.M. injections of 2 and 3 (x 10^9) EDV-COVID-αGC into BALB/c mice resulted in increased IFNα, IFNγ, IL-12-p40 levels 8 h post dose 1. (**I**) IL-2 levels in 2 x 10^9 and 3 x 10^9 EDV-CoV2-αGC particle dose after 8 h dose 1. (**J-K**) TNFα and IL-6 levels in 2 and 3 (x 10^9) EDV-CoV2-αGC particle dose after 8 h dose 1. (**L**) IL-21 levels for 3 x 10^9 dose level measured at day 28. (**M**) IL-10 levels in 3 x 10^9 EDV-CoV2-αGC particle dose after 8 h dose 1.

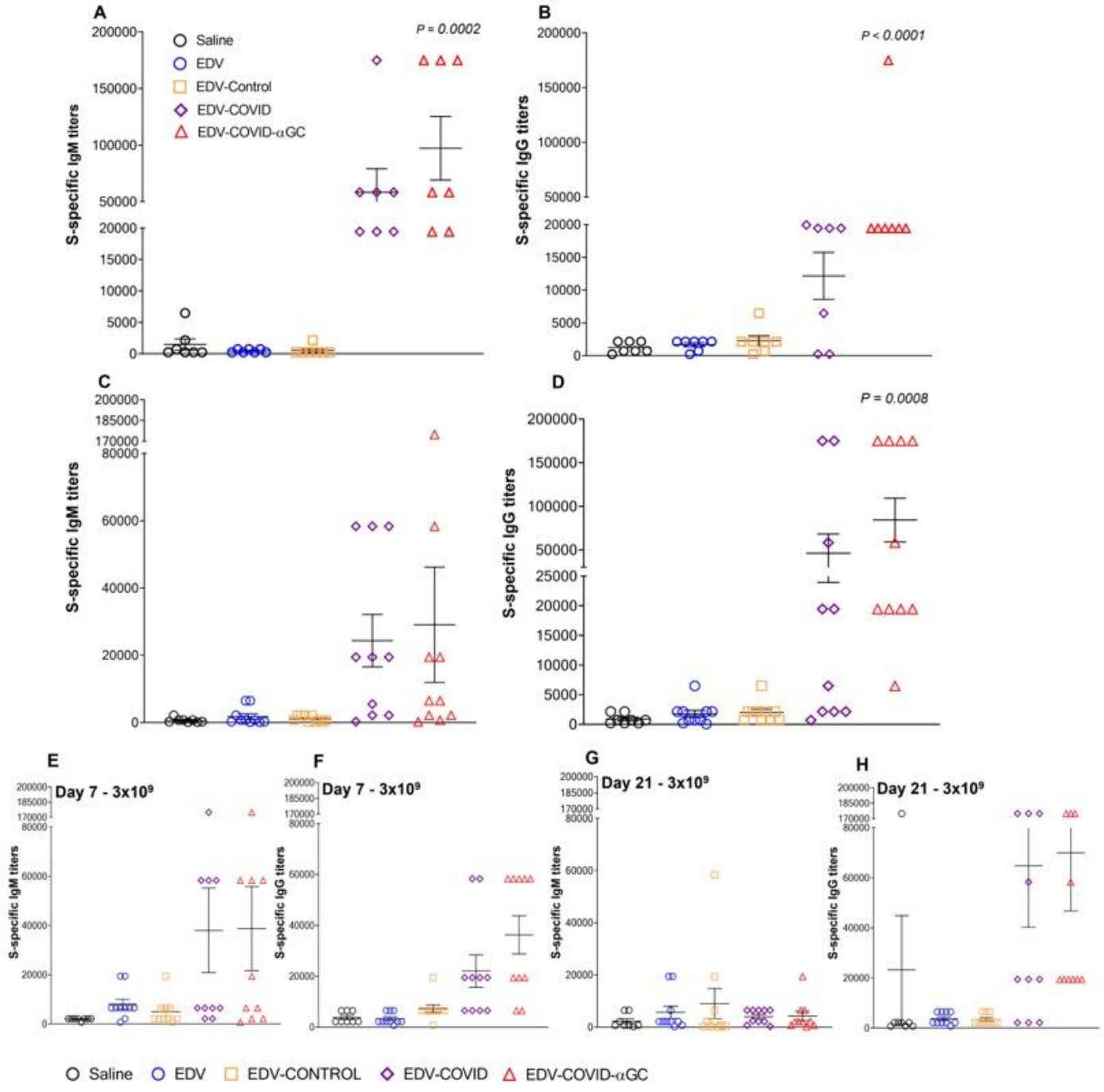

Figure 2

S-specific IgM and IgG titers. (**A-B**) Day 28 IgM and IgG S-protein specific titers for 2 x 10^9 and (**C-D**) 3 x 10^9 dose levels. (**E-F**) IgM and IgG S-protein specific titers for 3 x 10^9 dose at day 7 and (**G-H**) at day 21.

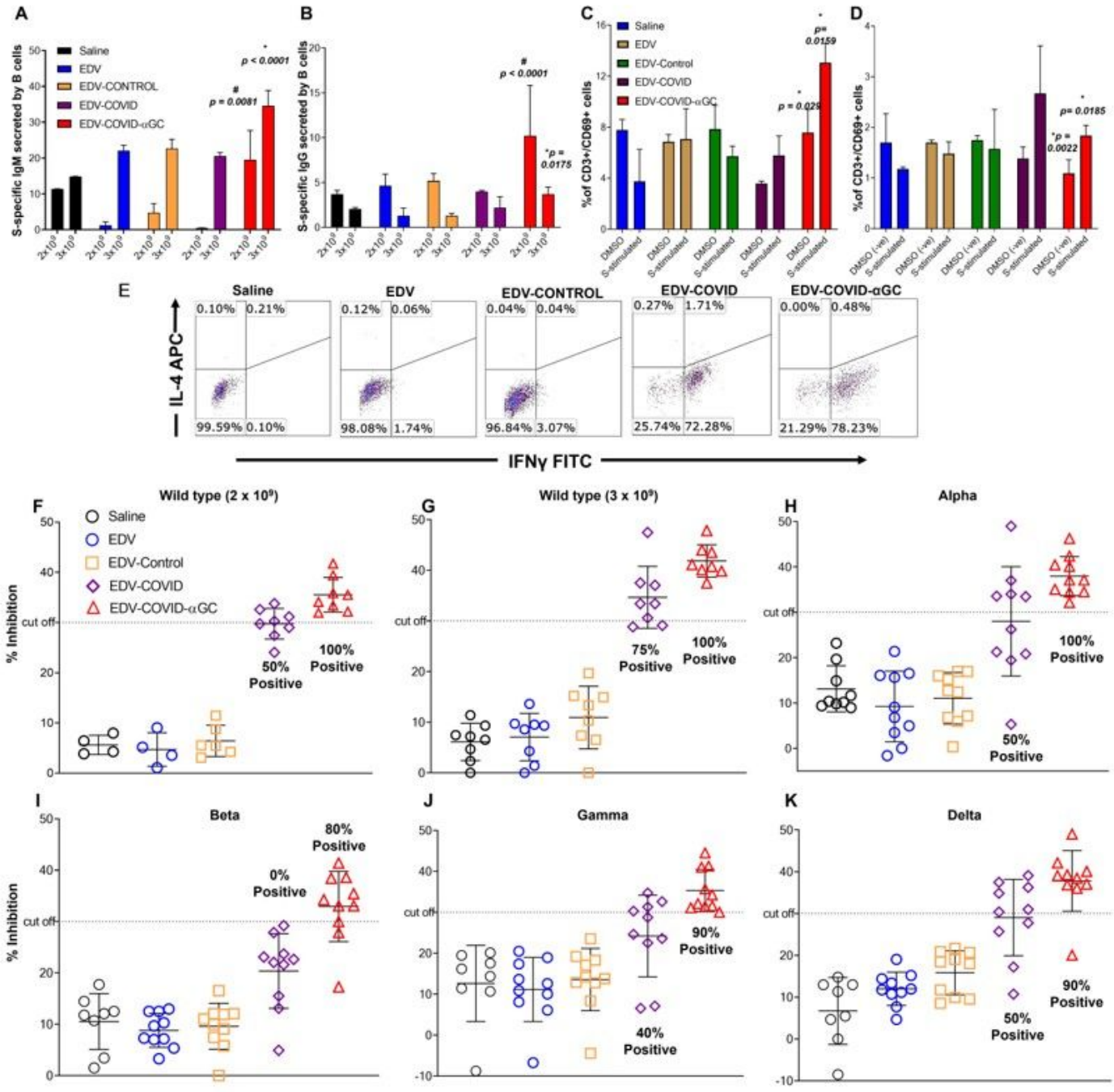

Figure 3

Ex-vivo **AIM Assay on murine bone marrow derived B cells and splenocytes and Surrogate Viral Neutralization Test (sVNT) on mouse serum.**

IgM (**A**) and IgG (**B**) S-protein specific titers from bone marrow-derived B cells isolated from 2 x 10^9 and 3 x 10^9 treated mice at day 28 post-initial dose after *ex-vivo* stimulation with SARS-CoV-2 S-protein. #: the difference was significant compared to all 2 x 10^9 injected mice; *: the difference was significant compared to all 3 x 10^9 groups. S-specific CD69 expression within the $CD8^+$ cytotoxic T cell population in 2 x 10^9 (**C**) and 3 x 10^9 (**D**) EDV immunized mice following the stimulation of *ex vivo* splenocytes using the SARS-CoV-2 S-protein. *: the difference was significant compared to DMSO (-ve) stimulated controls. Data presented as mean ± SEM. (**E**) IFNγ (Th1) and IL-4 (Th2) expression with the $CD3^+$ $CD4^+$ T cell population in SARS-CoV-2 S-protein stimulated *ex vivo* splenocytes. (**F-K**) Viral neutralization tests (VNTs) using the cPASS™ SARS-CoV-2 Neutralizing Antibody Assay (FDA approved) for detection in various species was used to assess inhibition of RBD binding to hACE2 receptor. (**F**) VNTs using the serum of 2 x 10^9 and (**G**) 3 x 10^9 EDVs immunized mice against SARS-CoV-2 RBD Wuhan Wild Type. Subsequent VNTs were conducted using the serum of 3 x 10^9 EDV immunized mice against the Alpha (**H**), Beta (**I**), Gamma (**J**) and Delta (**K**) variant RBDs.

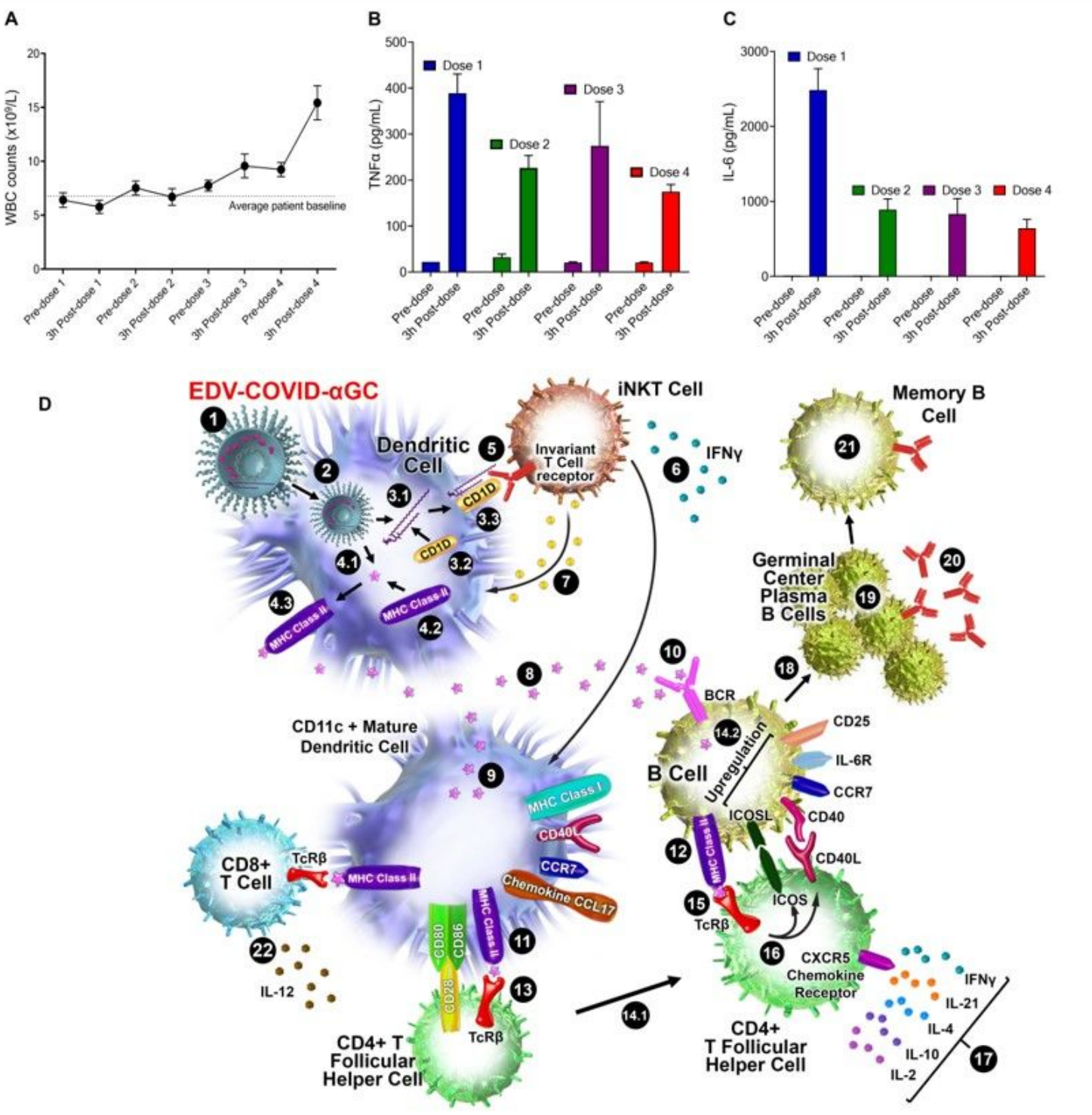

Figure 4

Patient immune response and schematic diagram of iNKT-licensed dendritic cell activation.

(**A**) WBC counts from 13 patients receiving 4 doses of EDV-αGC over a 4-week period. (**B**) Serum TNFα and (**C**) IL-6 levels of 13 patients receiving 4 doses of EDV-αGC over a 4-week period. Data presented as mean ± SEM. (**D**) Schematic diagram of iNKT-licensed dendritic cell activation; (1) EDV-COVID-αGC injected i.m. in mice, (2) phagocytosed by dendritic cells (DC), degraded in lysosomes, (3.1) αGC released from EDVs, (3.2) CD1d binds to αGC, (3.3) CD1d:αGC complex displayed on DC cell surface, (4.1) spike

polypeptides also released from EDVs, (4.2) MHC Class II binds to the S-peptides, (4.3) display them on same DC cell surface. (5) iNKT semi-invariant T cell receptor binds to CD1d/αGC complex, (6) rapidly secretes IFNγ which triggers upregulation of CD40 ligand in DCs inducing DC maturation/activation with increased costimulatory capacity through upregulation of CD80, CD86, CCR7, MHC Class I molecules, pro-inflammatory cytokine IL-12 & chemokine CCL17. (7) Binding of CD1d:αGC complex to the iNKT TCR triggers perforin release which kills the CD1d/αGC complex displaying DCs. (8) S-polypeptides are released from dying DCs, (9) endocytosed by activated CD11c+ DCs and (10) naïve B cells via B cell surface receptor, and (11, 12) displayed on each cell surface via MHC Class II. (13) MHC Class II/spike on DC surface binds to CD4+ TCRβ on CD4+ T follicular helper (T_{FH}) cells, and (14.1) these signals induce the T_{FH} cell differentiation and upregulation of chemokine receptor CXCR5 and downregulation of CCR7, which allows these cells to migrate to the T/B border. (14.2) B cells activated by S-polypeptide engagement of BCR increase CCR7 expression and migrates to the T/B follicle border in search of cognate CD4+ T cells. (15) Recognition of the S-peptide/MHC II complex on B cells by the TCRβ enables T_{FH} cells (16) to express CD40 ligand and ICOS and (17) secretes the cytokines IL-21, IFNγ, IL-4, IL-2, and IL-10. T_{FH} cells are strongly enriched for cells expressing the highest levels of IL-21. (18) this cognate help stimulates B cells to undergo intense proliferation, induction of Ig class switching, differentiation to plasma-like cells capable of secreting all major Ig isotypes. (19) Within GCs, B cells undergo somatic hypermutation and only B cells with the highest affinity antibody are selected. (20) These plasma cells secrete high affinity S-specific antibodies that can neutralize a variety of S-mutants. (21) These B cells differentiate into long-lived memory B cells. Throughout this process, IL-21 induces expression of CD25, enabling the B cells to respond to IL-2, also derived from T_{FH} cells, which promotes the effect of IL-21. Similarly, IL-21 induces expression of IL-6R on PCs, which allows these cells to integrate survival signals by IL-6. (22) DCs displaying S-peptides via MHC class II also elicit an S-specific CD8+ T cell response.

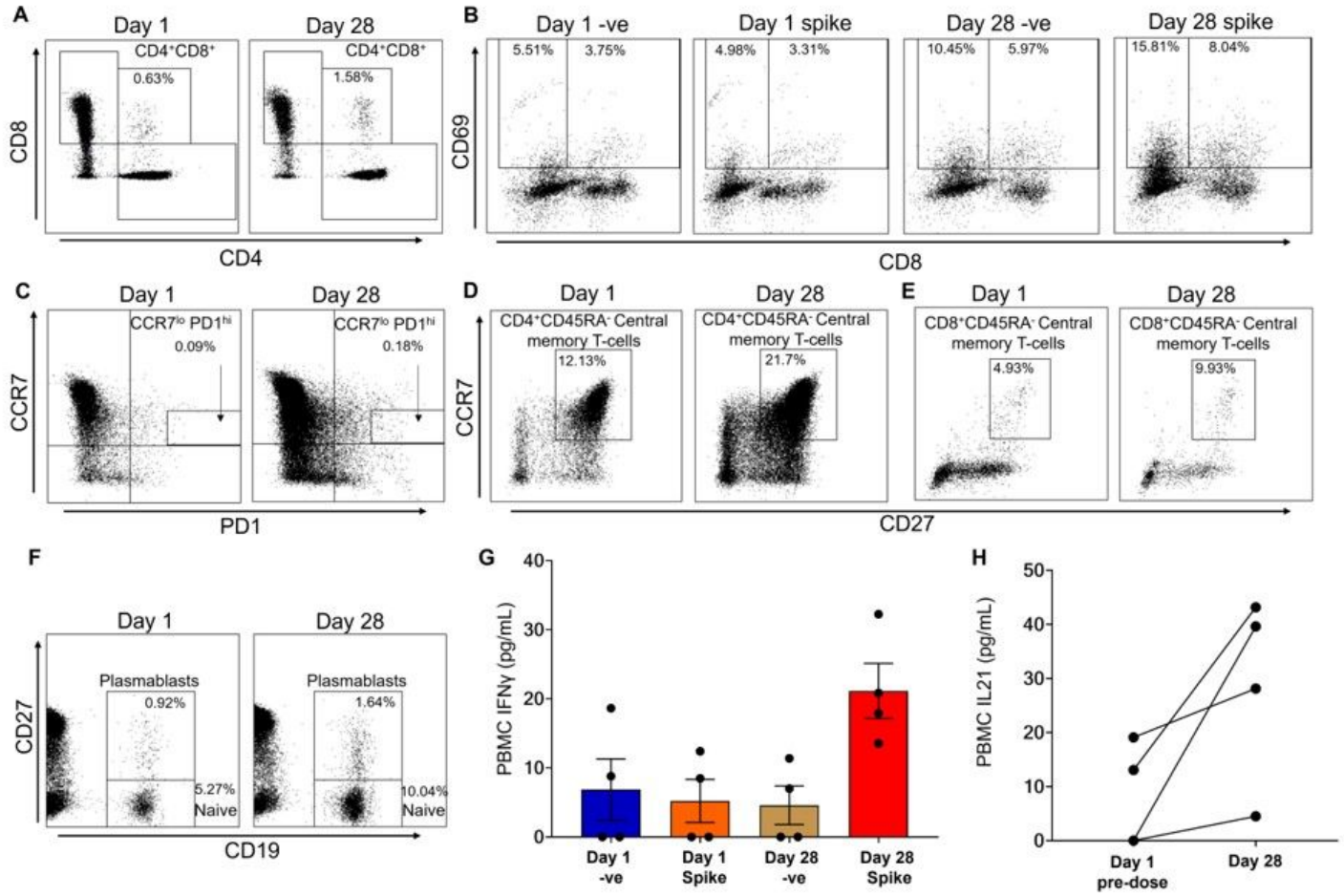

Figure 5

Data from the first 4 EDV-COVID clinical trial volunteers at 28 days post-initial injection.

An example of PBMC analysis (**A-E**) of CD4 CD8 co-positive population on day 1 and day 28 (**A**). CD8+ T cell activation following spike protein stimulation on day 1 and day 28 (**B**). (C) The presence of effector follicular helper T cells in PBMCs on day 1 and day 28. (**D**) The presence of central memory CD4+ T cells in PBMCs on day 1 and day 28. (**E**) The presence of central memory CD4+ T cells in PBMCs on day 1 and day 28. (**F**) A representative example of the presence of naïve B-cells and plasmablasts in PBMCs on day 1 and day 28. (**G**) IFNγ production of *ex-vivo* PBMCs following stimulation with SARS-CoV-2 S-protein. (**H**) Production of IL-21 from *ex-vivo* PBMCs from day 1 pre-dose and day 28.

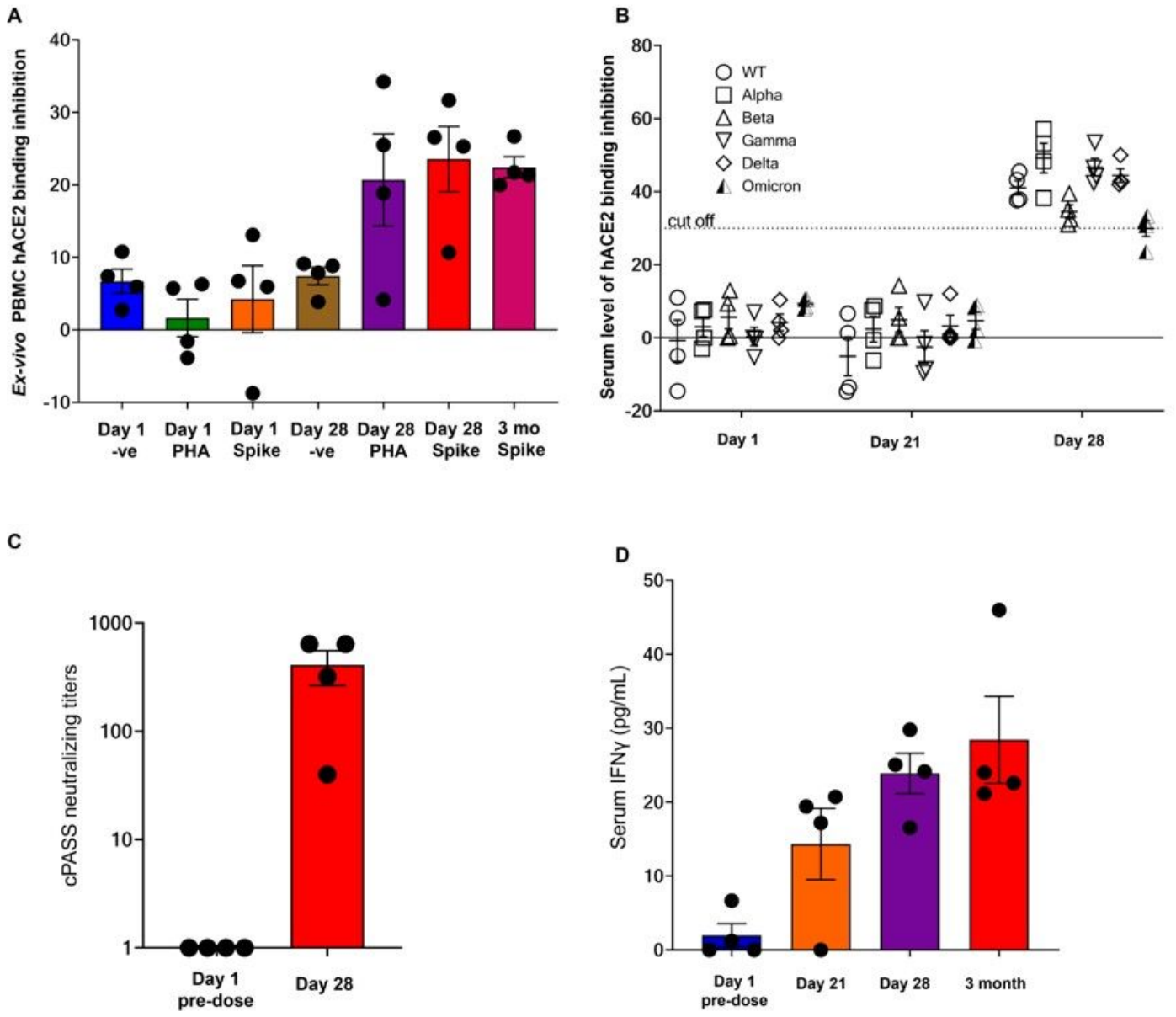

Figure 6

Neutralization data and serum IFNγ from the first 4 EDV-COVID clinical trial volunteers at 28 days and 3 months post-initial injection.

(**A**) The neutralizing effect of *ex-vivo* PBMC supernatant on SARS-CoV-2 RBD binding to hACE2 protein post-PHA or spike protein stimulation on day 1, day 28 and 3 months as analysed using the cPASS assay. (**B**) Surrogate virus neutralization assay again wildtype and Alpha, Beta, Gamma, Delta and Omicron variants from the serum of the first 4 healthy volunteers on day 1, day 21 and day 28. (**C**) Serum neutralizing antibody titers against the SARS-CoV-2 wildtype RBD. **(D)** Serum IFNγ levels of the first 4 healthy volunteers on day 1, day 21, day 28 and 3 months.

Supplementary Files

This is a list of supplementary files associated with this preprint. Click to download.

- GaoetalNatureBiotechSuppNBTRA56566.docx
- nreditorialpolicychecklist.pdf
- ReportingSummary.pdf